ISSN 1882-3432

TECHNOLOGY DEVELOPMENT CENTER NEWS
NATIONAL INSTITUTE OF INFORMATION AND COMMUNICATIONS TECHNOLOGY
Serial No. 33 September 2013

CONTENTS

(continued on inside front cover)

A Plan of the Automatic Observation System for the Tomakomai 11-m Radio Telescope

SORAI Kazuo (*sorai@astro1.sci.hokudai.ac.jp*), **MINAMIHARA Noriyuki, MOTOGI Kazuhito, OHISHI Yukie, HIURA Koichiro, UMEI Michiko, SEGAWA Yoko, TASHIRO Takami, SEKO Akifumi**

Department Physics / Department of Cosmosciences, Hokkaido University
Kita 10, Nishi 8, Kita-ku, Sapporo, 060-0810

Abstract: The Tomakomai 11-m radio telescope has been operated in 22-GHz band remotely from Sapporo about 70 km far away since the end of 2005. The telescope has been used for 1,500 to 4,000 hours per year, mainly for surveys of NH_3 molecular lines or monitors of H_2O maser toward the Galactic star-forming regions. Automatic observation system for the telescope is planed to make observation more efficiently. We have started to modify our programs for operating instruments and getting information on climate for preparation. Our plan of the new system is presented as well as the present status of the telescope.

1. Present Status

The Hokkaido University Tomakomai 11-m radio telescope (Fig.1) is settled in Tomakomai about 70 km far away from Sapporo. The telescope was modified from geodetic VLBI system in S/X bands to VLBI/single-dish system in 22-GHz band and operated remotely from Sapporo since the end of 2005[1].

Figure 1. Tomakomai 11-m radio telescope.

We have operated the telescope for 1,500 to 4,000 hours per year, mainly for surveys of NH_3 molecular lines or monitors of H_2O maser toward the Galactic star-forming regions in a single-dish mode, while for zero to 150 hours per year for VLBI observations.

One of the main observations using this telescope is a survey of dense molecular gas from which stars form in inversion transition lines of NH_3 molecule[1], in order to clarify whether distribution and physical properties such as temperature, density or star formation efficiency of dense molecular gas is different from one cloud to another. A recent NH_3 observation has revealed that dense molecular gas exists in the star-forming region G23.44-0.18 located near the end of the Galactic bar[2]. Two molecular clouds[3] seem to collide each other in this region, and the dense molecular gas is found just in the overlap region. An additional observation of $H^{13}CO$ line in higher spatial resolution and higher sensitivity with the Nobeyama 45-m radio telescope has suggested that the dense molecular gas formation was triggered by cloud-cloud collision[2].

2. Automatic Observation System

Our NH_3 lines survey takes long time for integration toward each observation position, since the telescope beam size of $\sim 4'$ is relatively larger than typical apparent sizes of the regions emitting the lines and thus beam dilution of the emission is severe. In order to find a way out of the situation that man power for observation restricts our results of the survey, we have a plan to develop observation system for our telescope that make our survey more efficient.

The concept of our automatic observation system is as follows (Fig.2). An observer checks the whole system including the telescope and instruments once in a day and executing an observation schedule file. Each schedule file consists of several observations, for example, the first observation targets the Orion region in NH_3 lines, the second one does the Taurus region in the same lines, the third one monitors some H_2O masers, and so on. The automatic observation system judges whether weather condition is suitable for observation or not and whether a target object is rising or not, when the observation schedule is executed. The system sets the instruments for each observation if the observation is possible to be done. Observation commands such as tracking a target, calculating the Doppler frequency, starting integration, and so on, are ordered at last. Status of the telescope and instruments is reported from the system. In addition, if some trouble has occurred, it is reported to

the observer through e-mail.

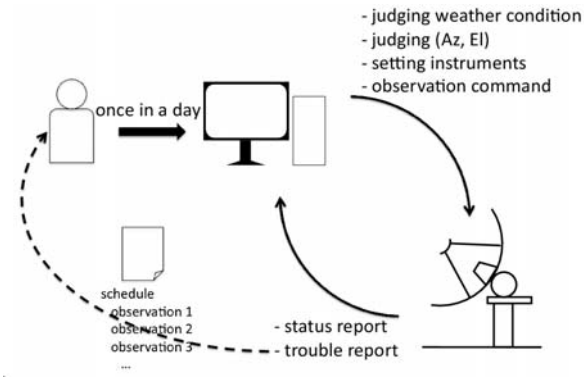

Figure 2. Schematic view of the concept of the automatic observation system for the Tomakomai telescope.

For developing the automatic observation system, we move the operating system from Windows to Linux in order to make communication among the computers which control several instruments easier. We have just made a new IF (intermediate frequency) instruments controlling system in Python and C on Ubuntu (Fig.3) and moved from the previous system in Agilent VEE Pro on Windows 2000. The new controlling system is very functional and operation speed becomes higher than the old system.

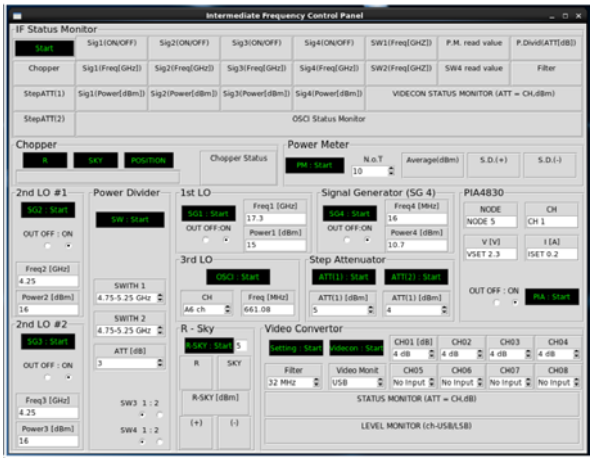

Figure 3. GUI of our new IF instruments controlling system.

3. Future Works

We make additional functions to the IF controlling system. Moreover, we have started making a new monitor system for weather conditions and status of the instruments. These system will be completed by the end of 2012. The most important development for our automatic observation system is making telescope controlling. We aim to test the new telescope controlling system at the end of the next March, however, developing the system may take longer time.

4. Acknowledgments

We acknowledge the Tomakomai Experimental Forest, Field Science Center for Northern Biosphere, Hokkaido University and the members of the Japanese VLBI Network. This project is financially supported in part by the National Astronomical Observatory of Japan.

References

[1] Sorai K., Habe A., Nishitani H., Hosaka K., Watanabe Y., Miwa S., Ohishi Y., Motogi K., Minamidani T., Awano J., Sumida S., Fukuya Y., Uchida R., Kaneko N., Fujimoto M. Y., Koyama Y., Kimura M., Nakai N. (2008), Large-Scale NH_3 Observations toward the Galactic Star-Forming Regions I. W51 Molecular Cloud Complex, Publications of the Astronomical Society of Japan, 60, 6, 1285–1296, 2008

[2] Ohishi Y., Sorai K., Habe A. (2012), Formation of Dense Gas and Stars near the End of the Galactic Bar, Publications of the Astronomical Society of Japan, 64, 4, *in press*, 2012

[3] Rathborne J. M., Johnson A. M., Jackson J. M., Shah R. Y., Simon R. (2009), The Astrophysical Journal Supplement, 182, 1, 131–141, 2009

Hope on GHz-band width signal recording and 100 k-channel spectroscopy for VLBI imaging of astronomical maser sources

Hiroshi Imai (*hiroimai@sci.kagoshima-u.jp*)
Graduate School of Science and Engineering,

Kagoshima University, 1-21-35 Korimoto, Kagoshima 890-0065, Japan

Abstract: High resolution and high dispersion spectroscopic imaging of astronomical maser sources with VLBI technique is a powerful tool for study on physical and dynamical structures of outflows and accretion of interstellar matter seen around dying stars and young stellar objects. Simultaneous mapping of multiple maser lines or some combination of maser line and continuum emission in VLBI should lead to a promising future in VLBI astronomy. Overcoming of a trade-off between wide band recording in VLBI backends and high dispersion spectroscopy in a correlator has been a long-term issue standing in front of such a future. Flexible digital filtering after high speed digital sampling as well as multi base band channel capability and its flexibility in signal correlation should be key technology, but nowadays in a realistic level. Here I show an example of possible future astronomical application of such technology to study on silicon-monoxide (SiO) maser sources associated with circumstellar envelopes.

1. Introduction

Simultaneous mapping observations of multiple spectral lines such as SiO $v = 3$, $v = 2$, $v = 1$ $J = 1 - 0$ maser transitions at rest frequencies of 42.5, 42.8, and 43.1 GHz, respectively, ammonia (NH_3) and water vapor (H_2O) masers at 23.7 and 22.2 GHz, respectively, hydroxyl (OH) and methanol (CH_3OH) masers at 6.0 and 6.7 GHz, respectively, and another OH maser and neutral hydrogen (HI) lines at 1.6 and 1.4 GHz, respectively not only improve the efficiency of the observations and their scientific outputs. They should provide great opportunity to compare the observed parameters of these emission (absorption for HI and sometimes OH) lines such as spatial and line-of-sight velocity distributions and intensities and to explore the physical and dynamical conditions of the target objects. As an example, Figure 1 shows the importance of simultaneous observations of SiO maser lines mentioned above. Furthermore, they enable to detect fainter maser lines by using the "phase-referencing technique" with the data of brighter maser lines for obtaining longer coherent exposure time. In fact, this technique is being adopted in the Korean VLBI Network now in a commission phase [6].

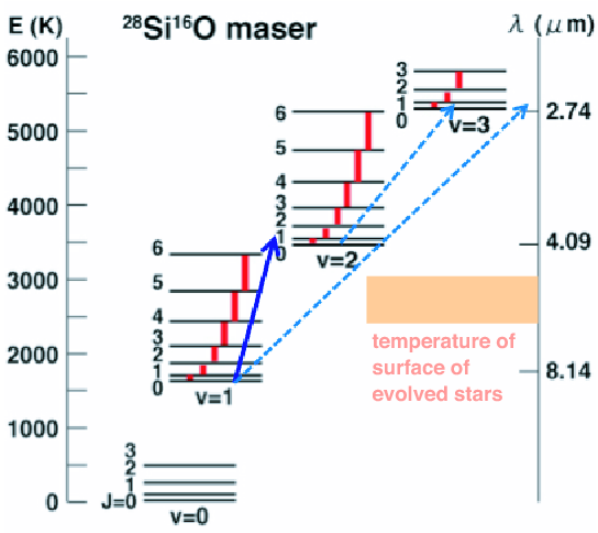

Figure 1. Energy level diagram of an SiO molecule. Thermal and maser transitions observed in interstellar gas clouds and circumstellar envelopes are presented by red lines. Solid and dashed arrows indicate the excitation of molecule through the "line overlapping" mechanism (e.g., [7]). This mechanism supposes that SiO molecules are excited by infrared emission from water vapor molecule in the circumstellar envelope. Note that the wavelength of the IR emission corresponds to the difference in energy levels between ro-vibrational states of SiO and can pump the SiO molecule so as to have an energy whose corresponding temperature is higher than that on the stellar surface. Alternatively, collisional excitation by shocks transferred from the stellar surface through stellar pulsation is also expected. These two different excitation mechanisms predict different performances of the different SiO maser lines at v =1, 2, and 3, e.g., spatial distributions and their temporal variations. They are currently observed in VLBI at 43, 86, and 129 GHz bands.

2. Demonstration of simultaneous VLBI observations of multiple SiO maser lines

We have demonstrated current capability of simultaneous VLBI observations of multiple maser lines using Japanese VLBI Network, in which four VERA 20 m, the NRO 45 m, and the NICT 34 m telescopes have taken part in the observations. One of such observations was reported in the paper [4]. Because a total band width is currently limited to 500 MHz in band pass filtering after down

conversion to the base band frequency, only two of the three SiO maser lines mentioned above can be simultaneously observed. Therefore, one pair of the maser lines are observed in one day, and other pair in the next day, eventually the total observation time is doubled. Due to *incompatibility* of high speed recording systems between VERA (DIR2000) and other two telescopes (e.g., K5), low speed recording system (DIR1000) should be used in order to obtain higher sensitivity for maser line observations with the NRO and NICT telescopes. As a result, estimation accuracy of group delay residuals is limited to ∼5 nsec due to too sparse monitoring of the residuals with only a bright calibrator. This causes a phase gradient of ∼1.5 turn of phase rotation between the two maser lines separated by ∼300 MHz when one applies the phase-referencing technique using the data of brighter maser lines to transfer their group delay solutions to the data of fainter maser lines. Furthermore, because the SiO masers are highly variable, even on a day scale, the *position reference* SiO $v = 2$ maser spot observed in both of two pairs of maser lines is also spatially unstable (σ ∼2 mas).

Figure 2 shows the obtained composite map of SiO v =1, 2, and 3 $J = 1-0$ maser lines towards the semiregular variable star W Hyrdae. Interestingly, only the $v = 3$ line has spatial offsets towards the central star with respect to other lines, suggesting the collisional excitation of the $v = 3$ maser line. However, when taking into account the relative position accuracy limited by the above-mentioned accuracy of estimated group delay residuals, these offsets are still on the level of marginal identification.

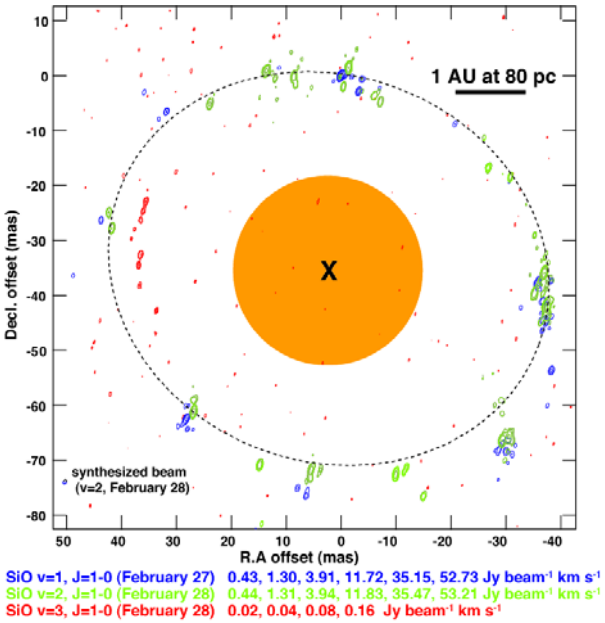

Figure 2. Comparison among the distributions of the SiO v =1, 2, and 3 ($J = 1 - 0$) maser emission observed in W Hya on 2009 February 27–28 for 2 × 6 hours [4]. The figure shows composite velocity-integrated maps of the SiO v =1, 2, and 3 masers. The contour levels are described at the bottom of the figure. The map origin is located at the $v = 2$ maser spot that was observed on February 28 and used as fringe-phase reference. A dashed line ellipse indicates a ring-shaped brightness morphology of the SiO v =1 and v =2 maser emission roughly fitted by eye. A orange circle indicates the size of the "radio photosphere" of the star [8].

3. Near future issues in wide-band spectroscopic VLBI observations

Thus, a high speed, wide bandwidth signal recording system is desired to observe the three maser lines at the same time. First of all, the bandwidth of the band pass filter in frequency down conversion should be expanded to 1 GHz or larger. The current baseband convertors as installed in VERA reduces the total bandwidth to 500 MHz. Because the upstream data of these down convertors have intermediate frequency (IF) signals at 5–7 GHz, the high speed sampler currently under development and in coming commissioning (in e.g., ADS3000+ and the OCTAVE system (OCTAD), Kawaguchi, N. in private communication) can be used for this down conversion and signal filtering.

On the other hand, even if the high speed recording system is available, the spectral resolution is insufficient in the current correlation system such as Mitaka FX correlator [1]. The requested total bandwidth and spectral resolution for the case of SiO maser observations described above (750 MHz and 16 kHz, respectively) exceed the specification of current correlators (16 784 and 1 024 spectral channels in Fourier transformation and correlation output, respectively, for Mitaka FX correlator). It is desired to obtain spectroscopic data from the whole receiving bandwidth in the uniform spectral resolution. However, the data analysis softwares and the architectures of end users' personal computers may not deal with a huge number of spectral channels, over 100 000 in the case of lower frequency band VLBI spectroscopy. In spite of absence of any spectral line in a specific frequency range, low frequency resolution data from such a frequency range is still necessary for detecting continuum emission of the target source. Thus the spectral resolution should be flexibly changed through the total bandwidth. Software correlation systems as developed in NICT and Swinburne University of Technology (DiFX, e.g., [5, 2]) should be quite flexible to these requirements.

Taking into account the trade-off between the wider bandwidth and sharper spectral resolution as discussed above, the technology of digital filtering (e.g. [3]) is still essential. Today, the total bandwidth in signal receivers and digital samplers is much larger than that with which VLBI correlators can deal (in real-time processing speed). The digital filter shall choose frequency ranges relatively essential for signal processing and transfer the filtered signals in moderate sampling rates to the correlators.

For VLBI spectroscopy, balanced development of receivers, samplers, digital filters, recorders, and correlators is quite essential. From the author's point of view as an astronomer, the current development environment of VLBI in Japan looks optimistically observable since starting the development of software correlation system [5]. The replacement of VERA's correlation system to a software correlator (Kimura, M. and Oyama, T., in private communication) in 2013 will approach the fruitful astronomical situation described above. Data analysis scheme that can process the correlated data produced under such a situation is under construction by the author[1], including pipeline processing scripts and maser spot finding algorithm.

4. Acknowledgment

HI was financially supported by Grant-in-Aid for Scientific Research from Japan Society for Promotion Science (20540234).

References

[1] Chikada, Y., Kawaguchi, N., Inoue, M., Morimoto, M., Kobayashi, H., & Mattori, S., The VSOP Correlator, Frontiers Science Series, Proceedings of the International VSOP Symposium held at the Institute of Space and Astronautical Science on December 5–7, 1989 and Proceedings of the mm-Wave VLBI Workshop held at the Nobeyama Radio Observatory on December 8–9, 1989, Tokyo, Japan, eds. Hirabayashi, H., Inoue, M., Kobayashi, H., Nishiniura, H., Okumura, S., Kuji, S., Sato, K., Asar, K., Sasao, T., & Kiuchi, H. (Universal Academy Press), p.369 (1991)

[2] Deller, A., Tingay, S. J., Bailes, M., & West, C., DiFX: A Software Correlator for Very Long Baseline Interferometry Using Multiprocessor Computing Environments, Publications of the Astronomical Society of the Pacific, 119, 318–336 (2007)

[3] Iguchi, S., Kurayama, T., Kawaguchi, N., & Kawakami, K., Gigabit Digital Filter Bank: Digital Backend Subsystem in the VERA Data-Acquisition System, Publications of the Astronomical Society of Japan, 57, 259–271 (2005)

[4] Imai, H., Nakashima, J., Deguchi, S., Yamauchi, A., Nakagawa, A., & Nakagawa, T., Japanese VLBI Network Mapping of SiO $v = 3$ $J = 1-0$ Maser Emission in W Hydrae, Publications of Astronomical Society of Japan, 62, 431–439 (2010)

[5] Kondo, T., Kimura, M., Koyama, Y., & Osaki, H., Current Status of Software Correlators Developed at Kashima Space Research Center, International VLBI Service for Geodesy and Astrometry 2004 General Meeting Proceedings. Ottawa, Canada, eds. Vandenberg, N. R., & Baver, K. D., NASA/CP-2004-212255, p.186 (2005)

[6] Kim, H.-G., Han, S.-T., & Sohn, B. W., The Korean VLBI Network Project, Exploring the Cosmic Frontier: Astrophysical Instruments for the 21st Century. ESO Astrophysics Symposia, ESO series, eds. Lobanov, A. P., Zensus, A. J., Cesarsky, C., & Diamond, P. J., (Springer-Verlag, Berlin and Heidelberg, Germany), p.41 (2007)

[7] Nakashima, J., & Deguchi, S., CORRELATION BETWEEN INFRARED COLORS AND INTENSITY RATIOS OF SiO MASER LINES, Astrophysical Journal, 669, 446–458 (2007)

[8] Reid, M. J., & Menten, K. M., IMAGING THE RADIO PHOTOSPHERES OF MIRA VARIABLES, Astrophysical Journal, 671, 2068–2073 (2007)

[1] see the wiki page of software repository of the Japan VLBI Consortium: http://milkyway.sci.kagoshima-u.ac.jp/groups/vcon_lib/wiki/9fbfd/Data_Analysis.html .

Present Status of Ibaraki station (Takahagi and Hitachi 32-m Radio Telescopes)

Yoshinori YONEKURA
(*y.yone@mx.ibaraki.ac.jp*)

Center for Astronomy, Ibaraki University
2-1-1 Bunkyo, Mito, Ibaraki 310-8512, Japan

Abstract: We briefly introduce the present status of the Ibaraki station as of 2013.

1. Introduction

Takahagi and Hitachi 32-m antennas, which have been used for satellite communications at 4 and 6 GHz by KDDI, were decommissioned in Mar. 2007. These antennas were handed over to NAOJ in Jan. 2009, and now belong to the Ibaraki station, which is a branch of Mizusawa VLBI Observatory of NAOJ. NAOJ and Ibaraki University, in cooperation with ISAS/JAXA, NICT, GSI, and universities (Hokkaido U., U. Tsukuba, Gifu U., Osaka Prefecture U., Yamaguchi U., and Kagoshima U.) have decided to use these antennas for Japanese and East-Asia VLBI network. We will use these antennas for single dish and 2-element interferometric observations as well as VLBI.

2. Renovation of Satellite-Communication Antennas into Radio Telescopes

The renovation of satellite-communication antennas into radio telescopes started from FY2009, and has been almost finished until FY2012 (Table 1).

The antennas themselves are not refurbished. Feed horn is newly developed for the observations at 6.7, 8, and 22 GHz. Antenna control system is newly installed.

We have been developing two cooled receiver systems for each antenna. One is covering 6.5–8.8 GHz (C/X-band), for observations of 6.7 GHz methanol masers and 8 GHz continuum. Two sets of C/X-band receivers have been completed. The other is covering 21–25 GHz (K-band), for observations of 22 GHz H_2O masers and continuum. In addition, K-band receiver is also used for single-dish observations of molecular lines as NH_3 and CCS. One set of K-band receiver have been completed, and the second set will be available within FY2013.

As for the VLBI backend, magnetic-tape recording system (so-called VSOP terminal, K4), 5 sets of K5/VSSP32 HDD recording system (32 MHz BW), and wide-band (500 MHz BW) HDD recording system (K5) are successfully installed. K5/VSSP32 can be used as a spectrometer system for single dish observations.

We succeeded first scientific VLBI imaging observations at 6.7 GHz in Aug. 2010. We also achieved "first fringe" in June 2012 between Takahagi and Tsukuba at 22 GHz using K5/VSSP32. We also succeeded test observations using wide-band (500 MHz BW) HDD recording system (K5) between Hitachi and Tsukuba at 8 GHz in Nov. 2012.

We are now testing two-element array using Hitachi and Takahagi antennas.

3. Performances of Telescopes

The system noise temperatures were measured to be ∼25 K and ∼50 K for the C/X and K-band, respectively, including atmosphere toward zenith.

The pointing accuracy is ∼0.3 arcmin, which is measured by the observations of strong radio continuum sources such as 3C273 at 8 GHz. The aperture efficiency at 6.7 and 8 GHz is measured to be 55–75% for Hitachi antenna, and 55–60% for Takahagi antenna. The aperture efficiency at 22 GHz is measured to be ∼30% at 22 GHz for both antennas. These performances are summarized in Table 2.

The location of the antennas are measured by using high-accuracy GPS measurement system (Table 3). These values are changed from the values[1] measured before "The 2011 off the Pacific coast of Tohoku earthquake".

4. Start of Scientific Observations using Single-Dish and Short-Baseline VLBI

As mentioned above, VLBI scientific observations have started in 2010. We recently started single-dish and short-baseline VLBI scientific observations. We have started single-dish observations to monitor the flux of methanol masers at 6.7 GHz from Dec. 2012 using Hitachi antenna. About 400 masers are observed more than once per 9 days. We also started daily short-baseline VLBI observations in order to monitor the flux of Sgr A* at 22 GHz from Feb. 2013 using Takahagi antenna among Mizusawa 10-m and Gifu 11-m antennas.

Acknowledgments

We acknowledge NICT for the use of correlation software. This work was supported in part by JSPS KAKENHI Grant No. 24340034.

References

[1] Yonekura, Y., IVS NICT-TDC News No.32, 24–25, 2011.

Table 1. Development status

	Hitachi	Takahagi
Single dish		
antenna control software	2009 Nov.	2012 Oct.
6–9 GHz cooled Receiver	2010 Aug.	2010 Dec.
22 GHz cooled Receiver	(2013)	2012 Dec.
spectrometer (K5/VSSP32)	2012 Mar.	2012 Mar.
VLBI		
with K4 recorder	2010 Aug.	2013 Mar.
with 500 MHz BW sampler+HDD	2012 Nov.	2013 Mar.
Two element array		
correlator	(2013)	

Table 2. Antenna performances

	6.7 GHz	8 GHz	22 GHz
Aperture Efficiency	0.55–0.75	0.55–0.75	$\sim$0.3
$T_{\rm sys}$* (@ $El = 90^\circ$)	25–30	25–30	50 (winter)–100 (May)
Beam size ($'$)	4.6	3.8	1.6
SEFD (Jy)	130–160	130–160	570–1150

Table 3. Antenna location (as of September 2012)

	X (km)	Y (km)	Z (km)
Hitachi	−3961.788796	+3243.597525	+3790.597709
Takahagi	−3961.881647	+3243.372513	+3790.687466
Distance between 2 antennas: 259.438 (m)			

Status report of the Tsukuba VLBI Station – damage of the antenna basement due to overloading –

Takahiro Wakasugi (*t-wakasugi@gsi.go.jp*)

Geospatial Information Authority of Japan
1 Kitasato, Tsukuba, Ibaraki 305-0811, Japan

Abstract: The Geospatial Information Authority of Japan (GSI) has carried out a lot of VLBI experiments in the Tsukuba VLBI Station, which was completed in 1998. We carried out 87 times of 24-hour session and 131 times of 1-hour session in last year. Thus, GSI has been contributing to the International VLBI Service for Geodesy and Astrometry (IVS). On the other hand, a lot of loads had been applied in the substructure of the azimuth rail. About five years ago, it was discovered that the phenomenon of the spurt of farinaceous matter from Grout of the antenna basement. It turned out that the situation of the antenna was very serious. In this paper, I report the state of the Tsukuba VLBI Station and inform a possible trouble of the substructure of antennas that have the wheel & track structure.

1. Introduction

The Tsukuba VLBI Station has a parabolic antenna with 32-m diameter and slewing speed of an unprecedented high mobility of 3 deg/sec in spite of its weight of 550 tons (Table 1.). It has been played an important role of VLBI experiments in eastern Asia after its construction in 1998 (Figure 1). However, the spurt of farinaceous matter from Grout was detected about five years ago and recently it seemed that the volume of the spurting matter increased acceleratingly.

Figure 2 shows the antenna substructure of the Tsukuba VLBI Station. The rail is mounted on the stiff metallic plate, which is called sole plate, and they are fixed on the basement concrete by some anchor bolts. The gap between the sole plate and the basement concrete is fulfilled by Grout, which is composed of the material like cement. It is considered that the frictional force due to the heavy usage made some parts of Grout farinaceous. Then, penetrated rain water weakened the strength of Grout furthermore, and finally farinaceous matter from Grout spurted out when a load of the antenna was applied (Figure 3).

The influence of the damage appeared in the results obtained by some experiments. In addition, according to the results of the pointing offset check with X band, it was emerged that the damage was getting worse rapidly from 2008, and it corresponded to the beginning of the spurt of Grout. The maximum azimuth offset versus the azimuth direction became about 0.06 degree (Figure 4) in the result of the pointing offset check in April 2013. The effect of the offset also appeared in the results of the correlation processing recently, and at last GSI had interrupted all experiments with the Tsukuba VLBI Station since May 2013.

Table 1. Specification sheet of the parabolic antenna of the Tsukuba VLBI Station

Parameter	Value
Height	36m
Diameter	32m
Weight	550t
Slew speed	3 deg/sec
Construction	1998

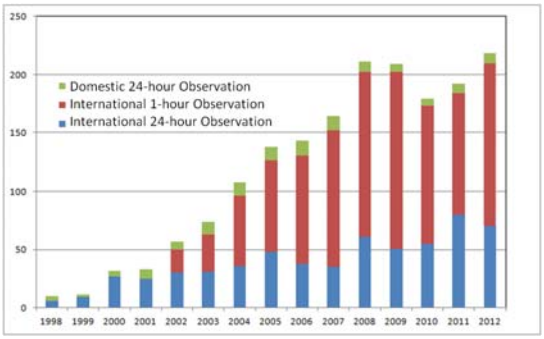

Figure 1. The number of annual experiments carried out in the Tsukuba VLBI Station after its completion in 1998. GSI has carried out approximately 200 times of VLBI experiments annually for the past several years in the Tsukuba VLBI Station.

2. Investigation of the Substructural Damage of the Antenna

We contacted the manufacturer of the antenna immediately to investigate the damage of the basement. Two kinds of investigations were carried out; first was measurement of the amount of subsidence of the sole plate against Grout by using dial gauges while the wheel was passing on. It was carried out at 117 points throughout the whole circumference. Second was direct observation of the actual state of the substructure by excavating Grout. Based on the subsidence result the excavation of Grout was carried out at four points. Three points were located where large subsidence was measured includ-

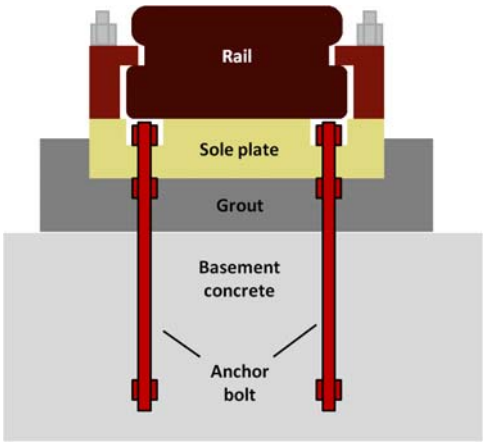

Figure 2. A schematic diagram of the antenna substructure of the Tsukuba VLBI Station.

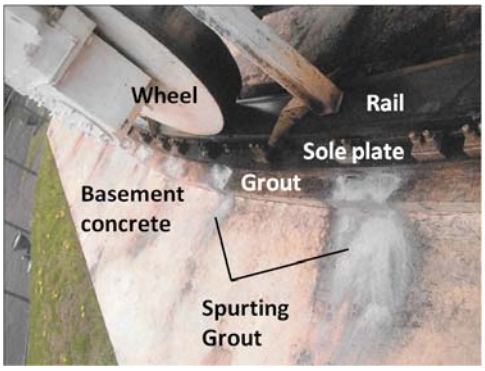

Figure 3. Photograph of the antenna substructure of the Tsukuba VLBI Station. Farinaceous Grout spurted out from the gap between the sole plate and Grout.

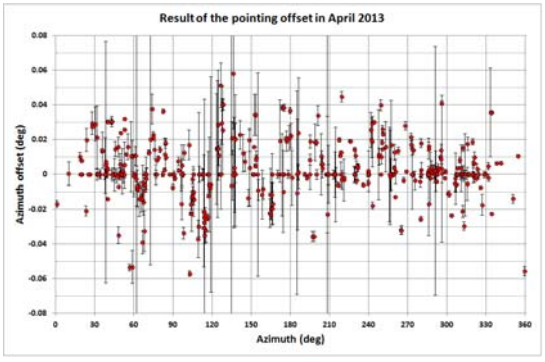

Figure 4. Result of the azimuth pointing offset check with X band versus the azimuth direction measured in April 2013. The maximum offset is approximately 0.06 degree.

ing the maximum subsidence, and another point was located where subsidence was never measured. The results of the investigations will be explained in the next paragraph.

3. Results of the Investigations

The result of the first investigation is shown in Figure 5. There were 9 points with larger subsidence than 2-mm, and the maximum subsidence was 3.5-mm. The amounts of gaps between the sole plate and Grout observed directly by excavating Grout corresponded to the results of subsidence obtained with dial gauges (Figure 6). On the other hand, the sole plate and Grout seemed to stand close each other at the excavated point where no subsidence was measured. These results implied that there were some gaps between the sole plate and Grout at the points where subsidence was measured.

I compared the results of subsidence and the pointing offset data with X band. When the antenna was oriented to the direction of the large pointing offset, three wheels were located on the rail where subsidence was larger than 2-mm (Figure 7). Similarly, when the antenna was oriented to another directions of the large pointing offsets, most of wheels were located on the positions with large subsidence. These results indicate that the results of the pointing offset check with X-band and subsidence with dial gauges are matching qualitatively. That is, when some of the wheels locate on the points with large subsidence, the subsidence of antenna causes the pointing offset. However, the subsidence of the antenna of 3.5-mm brings about the pointing offset of about 0.01 degree, so that the subsidence of 3.5-mm is not enough to explain the result of 0.06 degree maximum pointing offset. This means that it is insufficient for us to understand the actual state of the antenna basement only by the measurement of subsidence with dial gauges. Considering the amounts of gaps between the sole plate and Grout, there is a possibility that the rail and sole plate already subside due to their own weight although they doesn't take a load of the antenna.

4. Countermeasure and Future Plan

As I have just mentioned, the investigation of measurement of subsidence of the sole plate against Grout is not enough for us to know the actual state of the antenna substructure. Therefore we plan more investigation of the state of the antenna by measuring the level on the rail surface. After the investigation is finished, we intend to repair it with the best method derived from the results of all investigations. As one of the countermeasures, we

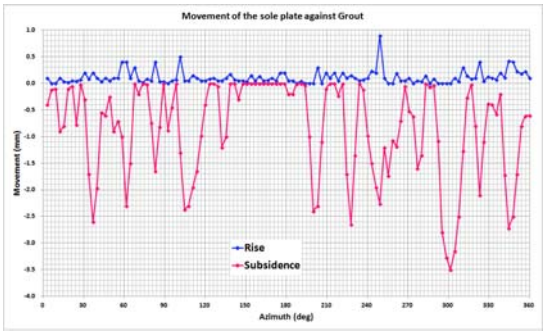

Figure 5. The results of the measured movements of the sole plate against Grout with dial gauges. The upper polygonal line indicates the amount of rise and the lower one shows the amount of subsidence of the sole plate against Grout. The measurement was carried out at 117 points throughout the whole circumference.

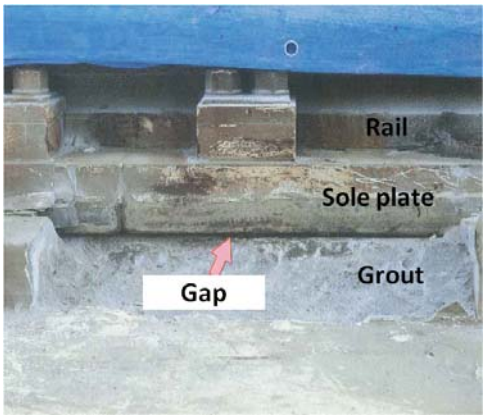

Figure 6. Photograph of the state of the antenna substructure after excavating Grout. The gap of a few millimeters was detected between the sole plate and Grout.

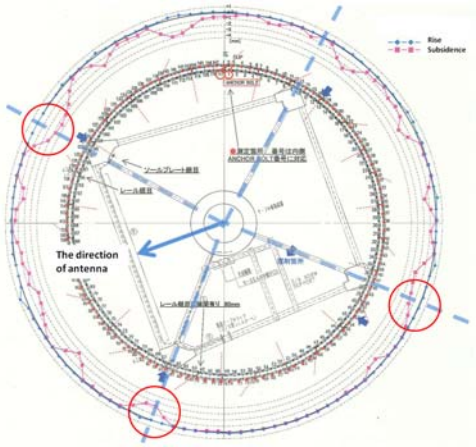

Figure 7. The locations of wheels when the antenna is oriented to the direction of the large pointing offset. The arrow signifies the direction of the antenna and wheels locate on four dotted lines. Three wheels correspond to the points where subsidence of the sole plate against Grout is large.

plan to inject new Grout of resinous material with keeping rail surface horizontal position. Finally, we aim to repair all damage and resume VLBI experiments as soon as possible.

5. Summary

It was emerged that the damage of the substructure of the Tsukuba VLBI Station was very serious. Because it had a bad influence on some experiments, we decided to cancel all experiments in the Tsukuba VLBI Station after May 2013. The results of the investigations showed that there were some gaps between the sole plate and damaged Grout, and the maximum subsidence was 3.5-mm. We plan to investigate the damage in more detail and aim to resume experiments after repairment of the antenna basement.

Development of Wide-band VLBI system (Gala-V)

Mamoru Sekido (*sekido@nict.go.jp*), **Kazuhiro Takefuji, Hideki Ujihara, Thomas Hobiger, Masanori Tsutsumi, Shingo Hasegawa, Yuka Miyauchi, Ryuichi Ichikawa, Yasuhiro Koyama, and Tetsuro Kondo**

Space-Time Standards Laboratory, Kashima Space Technology Center, NICT
893-1 Hirai, Kashima Ibaraki, Japan

Abstract: The project mission of our group is realization of compact VLBI system for precise frequency comparison between distant atomic frequency standards. For this mission, development of a new wide-band VLBI observation system named 'Gala-V' is in progress.

1. Introduction

Based on the needs of precise frequency comparison between atomic frequency standards at intercontinental distances, project of VLBI application for frequency comparison has started [1]. Takiguchi et al.[2] have made an experiment for comparison between VLBI and other frequency transfer techniques, such as Two-Way Satellite Time and Frequency Transfer (TWSTFT), GPS, and a special equipment (TCE) on Japanese Engineering satellite ETS8. They confirmed that VLBI has a potential of frequency comparison between distant atomic standards. Figure 1 shows results of another inter-comparison experiment between GPS common view, TWSTFT(Code phase), and VLBI. The data of VLBI measurements in the figure shows sum of estimated clock model polynomials and post fit residuals from CALC/SOLVE output. This experiment demonstrated that the precision of the measurement could be improved by increase of effective bandwidth of VLBI observation.

In the next step, we proceeded to develop a VLBI system with wide-band observation capability, which is semi-compliant with VGOS (VLBI2010 Global Observing System) specification. Transportable compact antennas are practically necessary to compare optical frequency standards in laboratories at distant location. For compensating disadvantages of small collecting area of the compact antennas, wide-band observation frequency range and combination with large diameter antenna are used for boosting the signal to noise ratio (SNR) of VLBI observations. Our wide-band observation system named 'Gala-V' employed a fixed frequency allocation in the frequency 3-14 GHz range,

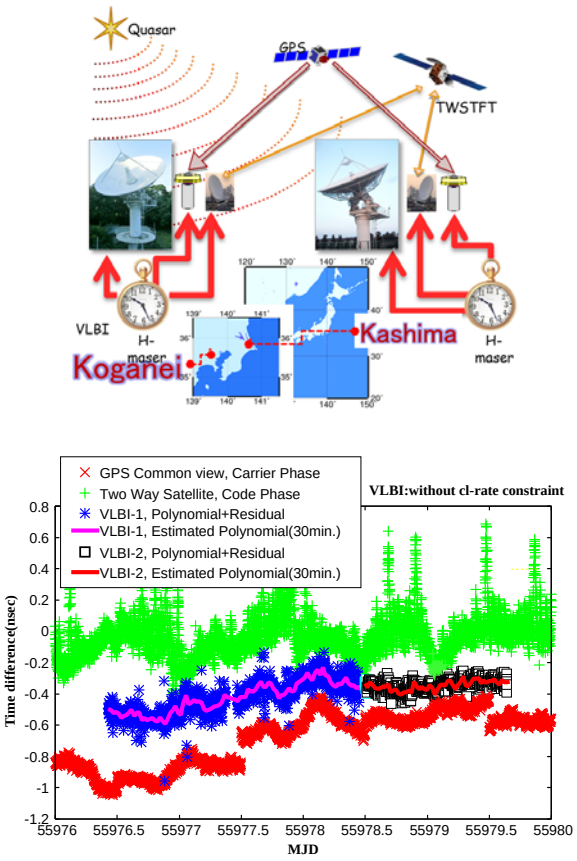

Figure 1. Experiment results of inter comparison of frequency transfer techniques (GPS Common View, TWSTFT Code, and VLBI). The experiment was conducted in Feb. 2012 between Kashima and Koganei 100 km distance. VLBI-1 and VLBI-2 are the continuous experiments with different frequency arrays. Eight X-band channels are spread over 500 MHz bandwidth in VLBI-1(''), and the same number of channels are allocated in 1 GHz bandwidth in VLBI-2('□'). Data sampling mode was 32Msps-1bit-16ch for both of two VLBI experiments. The result indicating that Weighted Root-Mean-Square (WRMS) of the residual were improved in case of wider bandwidth (VLBI-2) than the narrower case (VLBI-1).*

whereas the VGOS requires flexible frequency selection capability in the 2-14 GHz range.

2. RFI survey and Frequency Array

One of the reason of fixed frequency arrangement is due to technical restriction in designing wide-band feed system for 34m radio telescope, which is modified Cassegrain type. Full width of the viewing angle from the secondary focal point to the sub-reflector is 35 degrees, whereas popular wide band feed such as the Quad-Ridge Flared Horn (QRFH) has 60-120 degrees of beam width. Since newly de-

Table 1. Gala-V system parameters

Diameter of Antennas	34m, 1.6m, 1.5m
Observation Frequency	3500 - 4524 MHz
	5100 - 6124 MHz
	9900-10924 MHz
	13100-14124 MHz
Band width/Channel	1024 MHz
System Temperature	150-200 K
Effective Bandwidth	3.8GHz
Target Delay Precision	10 psec.

signing of a feed with narrow constant beam width over the wide frequency range will need long term research work, thus we decided to reduce the requirement condition of the VGOS specification for quickly realizing the multi-band observation system.

The frequency allocation was determined based on RFI (Radio Frequency Interference) survey, feed design condition, and consideration on delay resolution function. The RFI surveys were performed at Tokyo, Kashima, and Tsukuba. Figure 2 shows the results of survey made by max-hold method for 30 sec. in four horizontal directions (North, East, South and West). Since RFI was strong at lower frequency below 3 GHz, the survey was made by eliminating the signal at lower frequency with high pass filter (Fc=3.5GHz). Selected observation frequencies are indicated with rectangular boxes in Figure 2. Several RFI signals are still remaining in the observation bands, and they are to be suppressed by additional analog filters. Table 1 shows the current Gala-V system parameters. In the process to select the frequency of observation bands, feasibility of designing the multi-band feed was took into account. A prototype of the new multi-band feed is under development now, and it will be installed on the Kashima 34m antenna in this year. It is notable that frequency intervals of this array have a property of integer number of ratio 1:3:2 with multiple of 1.6 GHz. This is based on no-redundancy array theory[3], which enables fine delay resolution with minimum side-lobes. Good points in using fixed frequency array strategy are enabling quick development of the wideband VLBI system and quick catch up utilizing broadband delay observable. Its disadvantages are potential risk to be suffered from RFI, and limited compatibility in participating with VGOS observations.

3. Data acquisition and a RF Direct Sampler

The ADS3000+ sampler, which was developed under the collaboration among NICT, JAXA, and NAOJ, has the digital baseband conversion function. Two IF inputs with 1 GHz bandwidth signal are sampled at 2048 MHz at maximum, and following FPGA circuit works as digital filter for extracting arbitrary 16 × 32 MHz signals. The data stream of 2 × 2048 Mbps are recorded in each two PCs equipped with VSI-H interface card 'PC-VSI'. Therefore using four sets of ADS3000+ enables basic VGOS compatible observation, in which 16 channels of 32MHz band width are captured in the each band[4].

Table 2. Typical Parameters of K6/OCTAD-G ('GALAS') Sampler.

Sampling rate	16384 MHz
Typical output rate of samples per port	4096 Msps
Sampling quantization	3 bit
Output Quantization	1 or 2 bit
Number of output	4 ports
Output interface	10Gbit Ethernet 10GBASE-SR
Number of analog inputs	2
Max. input radio Frequency	16.4 GHz

Besides this VGOS compatible observation mode, a challenge of using RF (radio frequency) direct sampling technique is going to be tested in this development. Based on the success of the RF direct sampling experiment performed in 2011[5], a new sampler K6/OCTAD-G (code name 'GALAS') is under development. The K6/OCTAD-G has capability to sample the radio frequency signal at 16.384 GHz, then 4 × 1024 MHz signals are extracted by digital filter function. Each four data output stream comes out from four 10G-Ether ports separately in the VDIF data format in the UDP packet, or VDIF data with the header of VDIF Transport Protocol (VTP) over UDP. Thus any four RF signals with 1024 MHz bandwidth are captured from 16.4 GHz RF range simultaneously without analog frequency conversion. 2.

4. Compact Antennas and the last RHCP X-band VLBI Experiment

The compact transportable antennas developed by Ishii et al.[6] in the former project 'MARBLE' was equipped with the conventional S/X RHCP geodetic receivers, although they have been originally designed with the wideband observation system of 'VLBI2010' in mind. Wideband Quad-Ridge Horn antenna has been used at the feed system of the MARBLE. Therefore upgrading the MARBLE antennas by expanding the observation frequency region is the shorter way to realize Gala-

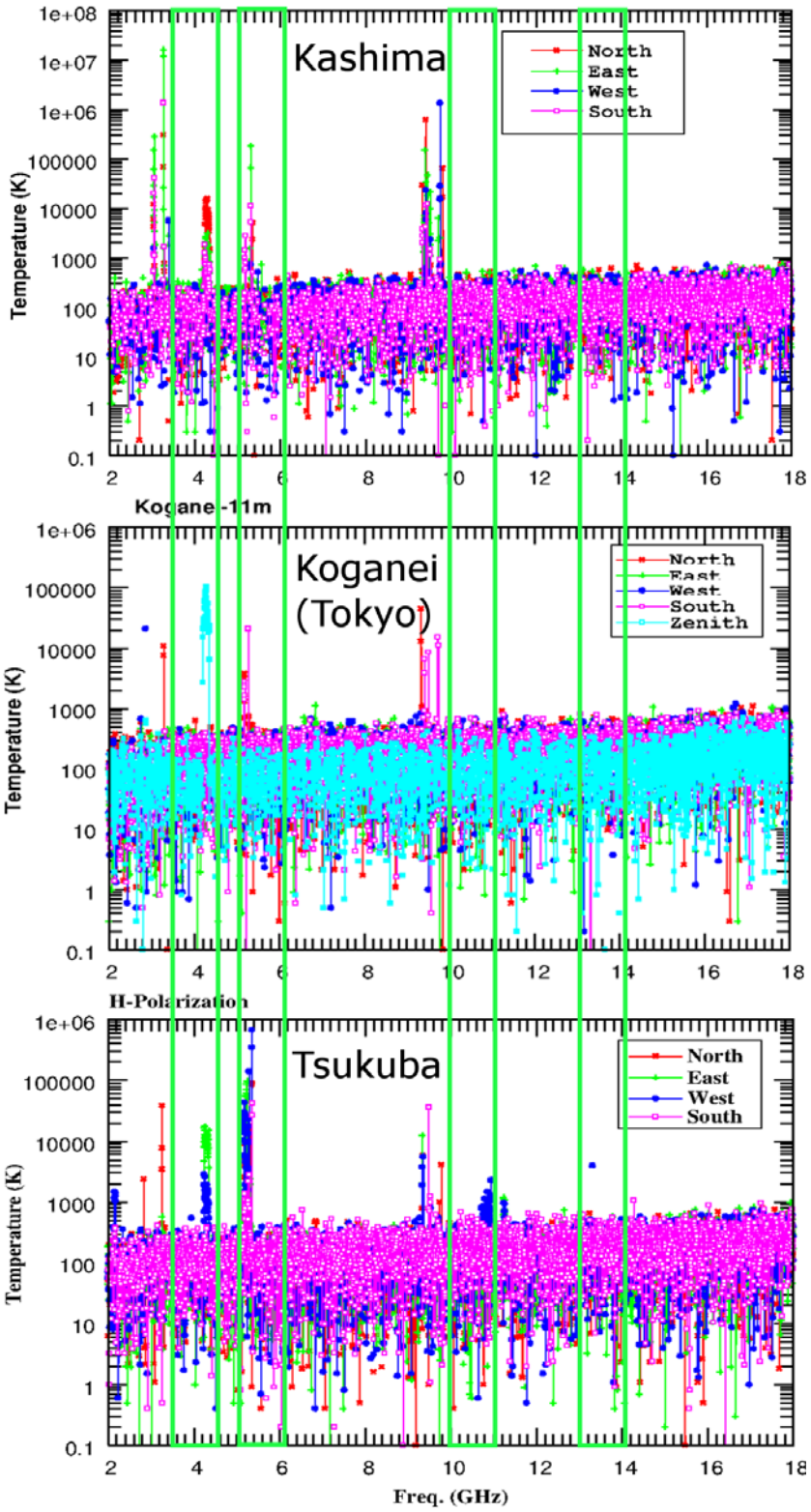

Figure 2. RFI survey (H-linear polarization, Horizontal 4 direction, Max-hold 30sec.) results for Kashima,Koganei(Tokyo) and Tsukuba. The measurements were made by using wide band receiver system with connecting high pass filter (Fc=3.5GHz) in front of the LNA. Four observation bands selected for Gala-V system are indicated by rectangular boxes.

Table 3. The result of X-band geodetic VLBI observation in Feb. 2013. Stations are MBL1:MARBLE 1.6m at Kashima, MBL2: MARBLE 1.5m at Koganei, Kas11: Kashima 11m, Kog11: Koganei 11m, Tskb32.

Post fit Residuals. X-station: Tskb32	Kas11	25 psec
	Kog11	24 psec
	MBL1	28 psec
	MBL2	26 psec
Coordinates [mm]	X:	-3997598292±3
	MBL1 Y:	3276714203±3
	Z:	3724293100±3
	X:	-3942062635±3
	MBL2 Y:	3368276235±3
	Z:	3702003846±3
SEFD Ratio w.r.t. Kas11	Kog11	2
	MBL1	200
	MBL2	300

V project. By the end of the second quarter of 2013, low noise amplifier (LNA) was replaced and circular polarization was changed to linear polarization to expand the observation frequency range. Signal down-link from the antenna to the observation room was also replaced from coaxial IF cable to wideband and optical RF transmission system 'E18000' developed by Sumitomo Osaka Cement Co. Ltd, which has flat characteristic over wide frequency range (1 – 18 GHz), low noise figure (NF $\leq$ 5 dB), and positive gain (G $\geq$ 30 dB).

Before these modifications, the last geodetic VLBI observation with the two MARBLE antennas was conducted in February 2013 together with 11m diameter antennas at Kashima and Koganei, and 32m antenna of Geographical Survey Institute (GSI). The aim of this experiment was two folds. One is to determine the terrestrial coordinates of the MARBLE antennas after the big earthquake of 2011. The second is to record the receiver performance before the upgrading for the Gala-V. S-band was not used in this experiment because of strong RFI coming into MARBLE antennas, which if vulnerable to RFI due to wider beam width. Thus ionospheric delay correction procedure was not applied, however its delay contributions were supposed to be negligible because of relatively short baselines. Table 3 shows the station coordinates and SEFD (System equivalent flux density) ratios with respect to that of Kashima 11m antenna estimated from the experiment data. Nominal SEFD of Kas11 is 5500 Jy.

5. Summary

Development of wideband VLBI system, which is semi-compliant with VGOS system, is in progress by upgrading the MARBLE system. The system is supposed to work in combination with wideband small diameter antennas and middle class antenna. Target of delay measurement precision with this system is at 10 pico seconds, and the keys to achieve this target are the wide effective bandwidth and boosting of SNR by joint observation with larger diameter stations. For quick catching up of the development, we have chosen four fix frequency bands for this project. Development of wideband multi-frequency feed for the Kashima-34m and RF direct sampling technique are the new challenges of the technology.

References

[1] Takiguchi, H., et al., Comparison with GPS Time Transfer and VLBI Time Transfer,IVS NICT-TDC News, No.28, 10-15, 2007

[2] Hiroshi Takiguchi, et al., Inter-comparison Study of Time and Frequency Transfer between VLBI and Other Techniques (GPS, ETS8(TCE), TW(DPN) and DMTD), IVS NICT-TDC News No. 32, 32–37, 2011.

[3] Moffet, A. T. , Minimum-Redundancy Linear Arrays, IEEE, Trans. Ant.&Prop., Vol.AP-16,No.2,pp172-185,1968.

[4] Chester Ruszczyk et al., VLBI2010 using the RDBE and Mark 5C, IVS 2012 General Meeting Proceedings, .81–85, 2012.

[5] T.Kondo, Success in an X-band VLBI using an RF direct sampling technique, IVS NICT-TDC News No. 32, 51, 2011.

[6] Atsutoshi Ishii, et al., Current status of development of a transportable and compact VLBI system by NICT and GSI, IVS NICT-TDC News No. 31, 2–5, 2010.

A status of the First Black Hole Imager, CARAVAN-SUBMM at 2012

Makoto Miyoshi
(NAOJ,*makoto.miyoshi@nao.ac.jp*)**,**
M. Sekido, Y. Koyama, H. Ujihara,
Y. Irimajiri (NICT), H. Ishitsuka,
S. Nemoto (IGP), Y. Asaki, M. Tsuboi
(ISAS), T. Kasuga (Hosei Univ.),
S. Nanbu, A. Tomimatsu (Nagoya Univ.),
M. Takahashi (Aichi Univ. Edu.), H. Saida,
S. Machiya (Daido Univ.) Y. Eriguchi,
S. I. Yoshida (Tokyo Univ.), S. Koide
(Kumamoto Univ.), R. Takahashi
(Tomakomai), T. Oka, J. Furusawa (Keio
Univ.), N. Kawaguchi, Y. Kato (NAOJ)
K. Niinuma (Yamaguchi Univ.),
T. Daishido (Waseda Univ), K. Wakamatsu
(Gifu Univ.) , T. Terasawa, M. Teshima
(ICRR), T. Kakimoto, Y. Tunesada
(TITEC)

National Astronomical Observatory, Japan,
2-21-1, Osawa, Mitaka, Tokyo, Japan 181-8588

Abstract: We here report the present investigations for the CARAVAN-SUBMM project.

1. Introduction

CARAVAN-SUBMM is a project constructing a sub-millimeter wavelength (submm) VLBI network at Andes for imaging and detecting black hole horizon and the surroundings that was never obtained before by any telescopes. It contains at least two fixed VLBI stations and one mobile VLBI station. "Mobile VLBI station" is a famous method in Japanese geodetic VLBI experiments since mid in the 1980s (Ichikawa et al., 2009). We apply the method in order to cover the u-v plain effectively and attain higher quality images at submm VLBI than those only fixed stations can do. By observing SgrA*, a super massive black hole at our galactic center, we aim imaging observations of the surroundings of the black hole horizon, and pave the way for verification of the general relativity and open observational black hole astrophysics (Miyoshi et al., 2011). Collaboration with the international ALMA increases the sensitivity and number of detectable sources. CARAVAN-SUBMM with world collaboration can realize the higher spatial resolution as well as 10 micro arc second order that ALMA alone never achieves. We report here the status of the project, CARAVAN-SUBMM at 2012.

2. Image Simulations

In order to image black hole horizon clearly, Miyoshi et al. 2004, 2007 have showed importance of shorter baselines around 1000 $\sim$ 2000 km at 230GHz. We performed further imaging simulations with changing model images and declinations of the target source. As the results we found following points:

1. It is quite difficult to resolve the true image using only the EHT configuration due to the lack of shorter baselines.
2. The difficulty still remains even if adding phased ALMA to the EHT array.
3. It is also difficult to obtain the disk shape around BH as a synthesized image using only CARAVAN-SUBMM array.
4. This difficulty still remains even if adding phased ALMA to the CARAVAN-SUBMM array.
5. It is possible to resolve the true image under the collaboration with the EHT and the CARAVAN-SUBMM.
6. Participating the phased ALMA to the above two-combined arrays will not dramatically enhance the image quality.

These results follow the common sense that image quality depends on how u-v plain can be covered. To resolve the true image around black hole horizon, we need not only longer baselines corresponding to the earth diameter but also shorter baseline around 1000 $\sim$ 2000 km at 230GHz. The essential role of phased-ALMA as a VLBI station is not the first detecting and imaging black hole horizon with VLBI but to increase the number of detectable sources with millimeter to sub millimeter VLBI.

3. Cost Down Study for Antenna

In order to realize the cost-down in making a high precision antenna panel for receiving millimeter to sub-millimeter wavelength, we examined the accuracy of the surface of antennas made by metal spinning method. Using an existing mold we could attain a surface accuracy as well as $60\mu m$ $r.m.s.$ easily. As the results, we found that the surface accuracy depends mainly on the accuracy of the mold surface. If we can use a higher precision mold in metal spinning, the more accurate the antenna surface will be obtained. The surface accuracy will reach as well as r.m.s. $30\mu m$ level if we use such a fine mold. The surface accuracy of the metal spinning antenna maintained within the 2 years of

our research period. Because the metal spinning antenna is very thin, the surface can be deformed easily by adding force non-uniformly. In practical use, a supporting structure of the antenna surface is very important to maintain the high accuracy of the surface.

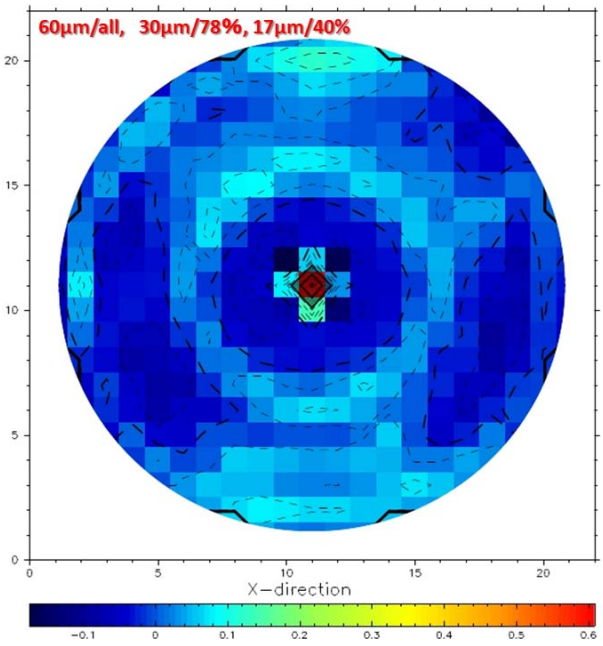

Figure 1. Surface accuracy measurement of a 90 cm antenna made by metal spinning method.

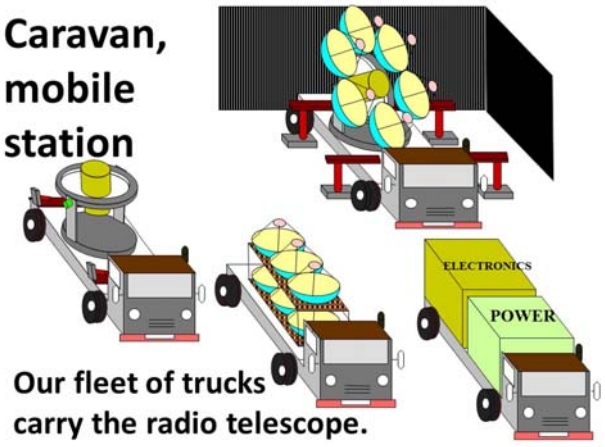

Figure 2. Mobile Station

Figure 3. Recent Survey Area

4. Mobile Station

Using several of very light antennas like those by metal spinning method, we can make a very light weighted radio telescope. As for telescope mount, a Japanese astronomer has already developed very light and low cost system(Kurita et al. 2004, 2009). Combining these we can make a radio telescope suitable for transportation along Andes mountains where road way is quite fully equipped today. The Caravan will contain not one but at least three of trucks. One for antenna carry, another for mount carry, and the other is for electric power-supply and recording electronics and hydrogen maser though we suppose power supply at operating telescope is commercial one. Among Peruvian Andes there are many cities and towns. Commercial based electric power supply is easily obtained.

5. Observing Site Survey

We plan to construct the fixed stations at around Huancayo Observatory (3300 m in altitude), IGP in Peru and at the Chacaltaya Cosmic Ray Observatory (5300 m in altitude) in Bolivia. Both observatories have a long-period collaboration with Japanese researchers. Including the two observatories, we performed site survey both in Peru and Bolivia for measuring the precipitable water vapor amounts. We used an infrared water vapor meter (Takato et al. in preparation) that is very small and easy to deal with. It has been used for surveying atmosphere in Antarctica, Tibet, and Atacama before. From 12th to 26th June in 2012, two persons attended to the survey from Japan, joined the IGP team, and performed the survey. They investigated two areas. One is an area along the road from Lima to Huancayo city including Huancayo observatory and COSMOS observatory (old solar observatory constructed by M. Ishituka). The other area is along the road from La Paz in Bolivia through southern side of lake Titicaca to city Tacna in Peru. Tentative PWV values are about 10 mm at Huancayo (Peru, 3314m), about 4 mm at Cosmos(Peru, 4600m) about 1.5 mm at Chacaltaya(Bolivia, 5300m) and about 1.2 mm at southern desert area (Peru, 4600m). Chacaltaya and the

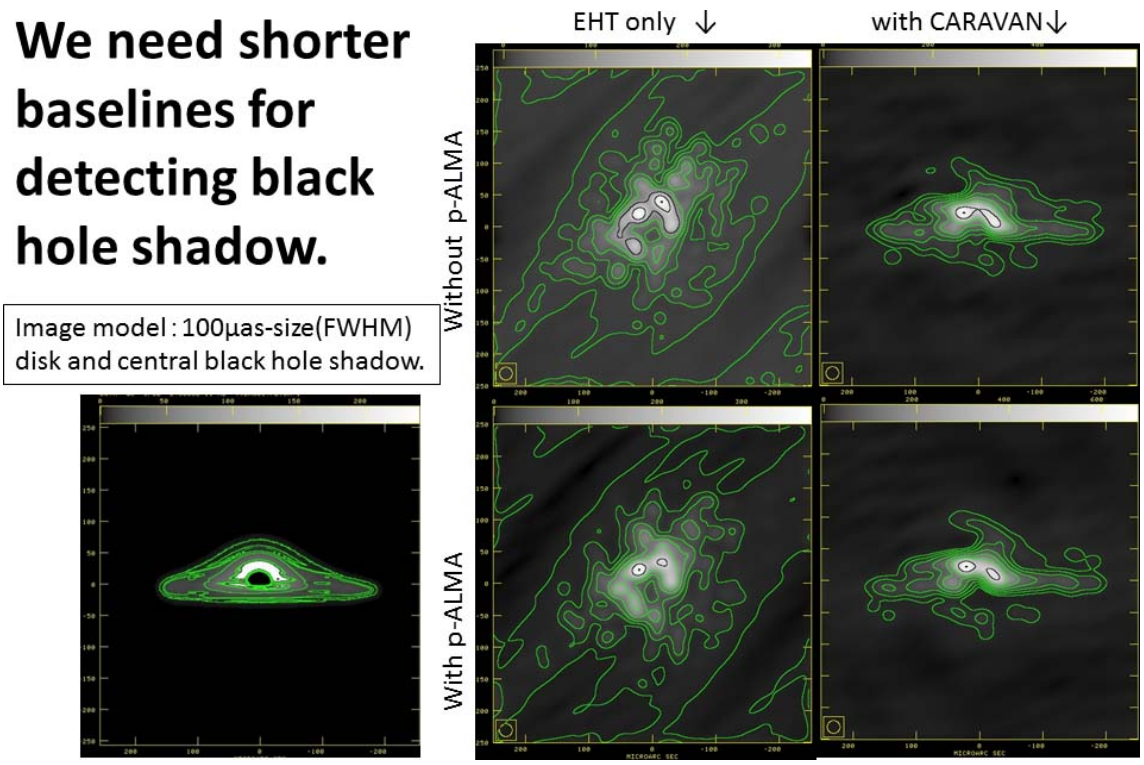

Figure 4. Imaging simulation. EHT observation(Longer Baselinesj alone fails to find intrinsic shape of the model image, though a false-shadow can be obtained. A better image can be obtained with Japanese CARAVAN-SUBMM. Phased-ALMA has little contribution to the shadow image detection.

southern Peru area show excellently low PWVs as well as those at ALMA site. Next step we plan to perform all season monitor at the two observatories. Also Huascaran, a north area of Peru must be surveyed.

References

[1] Miyoshi, M. et al., A First Black Hole Imager, Caravan-sub at Andes, 2011ASPC,4 39, 279M (2011)

[2] Ichikawa, R., A. et al., IVS NICT-TDC News No.30, (2009)

[3] Miyoshi, M. et al., PTPS, 155,186-189, (2004).

[4] Miyoshi, M. et al., PNAOJ, 10, 15-23, (2007), or astro-ph/0809.3548

[5] Kurita, et al.,"Ultra-Lightweight Telescope Mount", PASP, Vol. 121, Issue 877, pp.266-271(2009)

[6] Kurita, et al., "Development of the ultralight medium-size telescope", 2004, SPIE, Volume 5495, pp. 518-525(2004)

Flux monitoring observations of Sgr A* at S/X bands with the NICT Kashima–Koganei VLBI System

Shunya Takekawa[1] (*shunya@z2.keio.jp*), **Tomoharu Oka**[1], **Mamoru Sekido**[2]

[1] *Department of Physics, Faculty of Science and Technology, Keio University*
3-14-1 Hiyoshi, Kohoku-ku, Yokohama, Kanagawa, Japan
[2] *Space-Time Standards Laboratory, Kashima Space Technology Center, National Institute of Information and Communications Technology*
893-1 Hirai, Kashima, Ibaraki, Japan

Abstract: A compact radio source Sgr A* is the nucleus of our Milky Way Galaxy, harboring a supermassive black hole with mass of $4 \times 10^6\ M_\odot$. While the current activity of our Galactic nucleus is extremely low, an activation subsequent to the infall of the G2 cloud is expected within several years. In order to catch the flux variations associated with the G2 event, we have conducted flux monitoring observations of Sgr A* at S-band (2 GHz) and X-band (8 GHz) using the NICT Kashima-Koganei VLBI system since the middle of February 2013. We observed Sgr A* for 38 days in total, about five hours each day. Four quasars are also observed as flux calibrators. The X-band flux density was 0.48±0.05 Jy (preliminary), while S-band emission has not been detected. No significant change nor variation has been detected in the X-band flux density of Sgr A* yet. We intend to continue these monitorings as often as possible until at least May 2014.

1. Introduction

Most galaxies have supermassive black holes (SMBHs) at their centers, and some of them are observed as active galactic nuclei (AGNs). Our Galaxy also has a $4 \times 10^6 M_\odot$ SMBH at its center, which is recognized as a compact radio source Sgr A*. Despite its huge mass, Sgr A* is extremely dim and quiet. The bolometric luminosity of the nucleus is only $\sim 10^{33-35}$ erg s^{-1}, which is far below the Eddington luminosity of 6×10^{44} erg s^{-1}. This extreme dimness suggests a very low mass accretion rate ($< 10^{-5} M_\odot$ yr^{-1}), and thereby a low radiation efficiency. On the other hand, the widespread ($\sim$ 200 pc) distribution of Fe 6.4 keV fluorescent line emission implies that Sgr A* was far brighter ($\sim 10^{39}$ erg s^{-1}) than now about several hundred years ago[1]. It is possible that AGN activities are transient in general and currently inactive Sgr A* may be active sometimes. Such variations may be caused by intermittent accretion of interstellar gas onto the central SMBH.

Recently, the Max-Plank-Institute für extraterrestrische Physik (MPE) group has reported the discovery of a dense gas cloud, G2, which is on its way toward Sgr A*[2] (Figure 1). This cloud's mass is approximately three times as the mass of the Earth. The G2 cloud is on the elliptical orbit with high eccentricity (Figure 2) and thought to reach the pericenter, $\sim$ 2000 Schwarzschild radii from the nucleus, in Spring 2014[3]. The G2 cloud has been stretched and will be disrupted by the strong tidal force from the central SMBH. Some fraction of disrupted cloud will infall toward the nucleus, increasing the mass accretion rate on to the SMBH. This increase in the mass accretion rate is expected to cause a significant flare in all wavelengths. This G2 event provides a unique opportunity to witness a gas infall toward a SMBH. Thus, a number of groups are conducting and planning to observe this event in every wavelength [4].

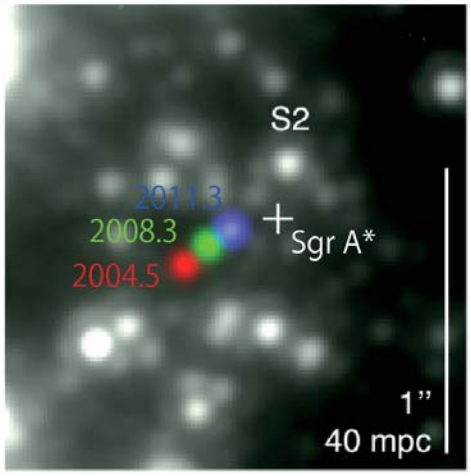

Figure 1. The infrared image of the central 1" of the Galaxy, taken by the MPE group[2]*. Color show the Br-γ images of the G2 cloud of four different epochs (red: 2004.5, green: 2008.3, blue: 2011.3) overlaid on the K_s-band image at 2011.3.*

2. Observations

In order to catch the radio flux variations associated with the G2 event, we have conducted flux monitoring observations of Sgr A* using the NICT Kashima-Koganei VLBI system since the middle of February 2013. This VLBI system consists of two

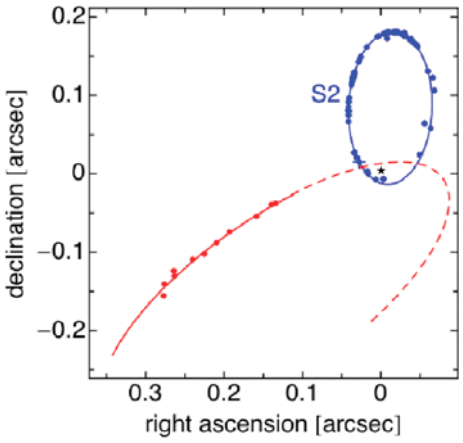

Figure 2. The orbit of the G2 cloud determined by the MPE group[2]. The small black star indicates the position of Sgr A. Red points show observed position of the G2 and red dotted line is its orbit. Blue line shows the orbit of the S2 star, of which the pericenter has been the nearest to the nucleus.*

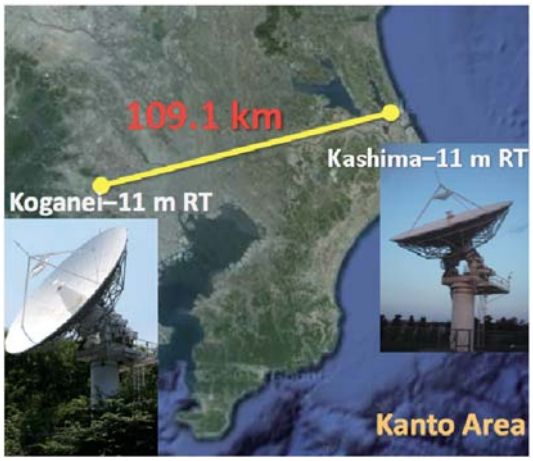

Figure 3. NICT Kashima-Koganei VLBI system.

11-m diameter antennas located at Kashima and Koganei, and K5/VSSP32 samplers. Locations of these antennas are shown in Figure 3. The baseline length is 109.1 km. Observing frequencies are S-band (2.21–2.29 GHz) and X-band (8.2–8.5 GHz). Thus, the spatial resolutions of this VLBI system are $\simeq$ 280 mas and $\simeq$ 70 mas at S and X bands, respectively.

In radio range longer than mm-wave, it is known that the apparent size of Sgr A* is roughly proportional to the square of observing wavelength, i.e. $\Delta\theta_{\rm mas} \sim \lambda^2_{\rm cm}$. This behavior is explained by the electron scattering in the line of sight[5]. Because of this, short ($\sim$ 100 km) baseline is sufficient for the cm-wavelength VLBI observations of Sgr A*.

Until 16 August 2013, we observed Sgr A* for 38 days in total, about five hours ($EL > 15°$) each day. Since 78th day-of-year (DOY), four quasars (NRAO 530, PKS 1622−253, PKS 1622−297, PKS 1921−293) are observed as flux calibrators, while only NRAO 530 had been used before 78th DOY. The integration times are, 300s, 30s, 240s, 240s, and 30s, for Sgr A*, NRAO 530, PKS 1622−253, PKS 1622−297 and PKS 1921−293, respectively, in each observing sequence. All the source were observed by turns.

3. Results

Figure 4 shows a plot of observed correlation amplitude of Sgr A* at X-band. No significant emission at 2 GHz have been detected. Using the correlation amplitude of NRAO 530, and its X-band flux of 3.3 Jy, we obtained the Sgr A* flux by,

$$S_{\rm SgrA^*} = 3.3\ {\rm Jy} \times \rho_{\rm SgrA^*}/\rho_{\rm NRAO530}, \qquad (1)$$

where $\rho_{\rm SgrA^*}$ and $\rho_{\rm NRAO530}$ are the correlation amplitudes averaged over each observing day. Fluxes of the other calibrators were calculated in the same way. Note that quasars are variable in every wavelength, thus the flux calibration method employed here is a bit controversial. Nevertheless, the X-band flux of Sgr A* is really stable, exhibiting no significant flare or variation. We obtained the average X-band flux is 0.48±0.05 Jy as a preliminary value.

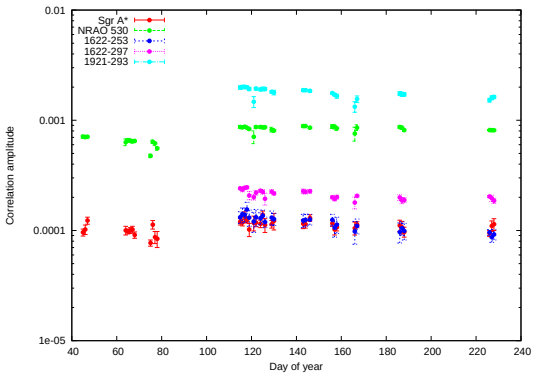

Figure 4. Correlation amplitudes of observed sources at X-band. These amplitudes are values averaged over each observing day. Error bars represent 1σ standard deviation for each day.

4. Summary

In order to catch radio flux variations of Sgr A* associated with the G2 event, we have conducted the flux monitoring observations at X-band and S-

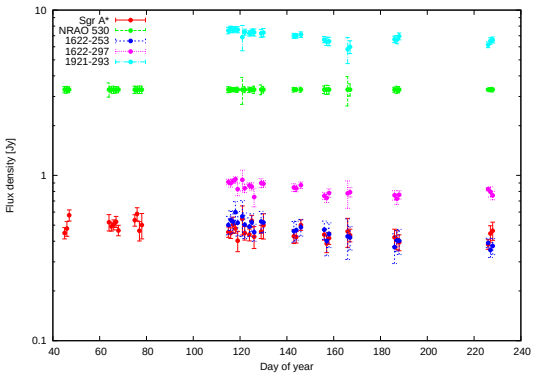

Figure 5. Calibrated flux densities of target sources at X-band. These flux densities are calculated by assuming that the flux density of NRAO 530 is stable (3.3 Jy) during the observing period. Error bars are 1σ standard deviation for each day.

band with the NICT Kashima-Koganei VLBI system. We obtained the X-band flux of Sgr A* from the mid-February to 16 August 2013 for 38 days, and measured a very stable value of 0.48±0.05 Jy. These monitoring observations are very important for studies black holes and AGNs. When the flare is detected in our monitorings, we will alert it to the world as soon as possible. We intend to continue these monitorings as often as possible until at least May 2014.

References

[1] Ryu, S. G., et al. 2012, AIP, 1427, 284R

[2] Gillessen, S., et al. 2012, Nature, 481, 51

[3] Gillessen, S., et al. 2013, arXiv:1306.13

[4] Gas Cloud Wiki; Observing proposals for 2013 (https://wiki.mpe.mpg.de/gascloud/ProposalList)

[5] Bower, et al. 2006, ApJ, 648, L127

The Study of Time Synchronization over VPN

Yusuke Kito (*y_kito@fjtakalab.dnj.ynu.ac.jp*),
Fujinobu Takahashi , *Faculty of Engineering,*

Yokohama National University
75-1, Tokiwadai, Hodogaya, Yokohama,
Kanagawa, Japan

Abstract: This paper presents the application of the new time synchronization protocol, PTP (Precision Time Protocol), and the verification result of that over the Internet. Some use NTP (Network Time Protocol) for the time synchronization through the Internet, but NTP is not accurate enough for the systems dealing with the time stamp like the financial transactions, the industrial field, and the next generation communications. PTP is also called IEEE 1588 and it will be of help in such situation. We have verified the accuracy of PTP time synchronization over VPN (Virtual Private Network) and LAN (Local Area Network).

1. Introduction

Time synchronization is popular technology for us like NTP. A computer's clock is managed by the crystal oscillator on the motherboard. Since tt is accurate but does not have enough stability, time synchronization is used for that. PTP is the protocol for the hardware clocks synchronization that is called IEEE 1588[1]. It is said that PTP is more accurate than NTP that is popular for us as the time synchronization protocol. Although NTP is not accurate enough for the systems dealing with the time stamp like the financial transactions. It is because that such systems have the computers exchange and storage the data including time stamp and it is dealt with the data in increments of one micro second. Hence PTP is the expected technology as the accurate time synchronization system dealing with the time in increments of one nano second and it will be of help in such situation.

2. PTP (Precision Time Protocol)

2.1 Basic Method

Figure 1 shows the basis of PTP time synchronization[1]. As the figure Master sends Sync Message to Slave, then Slave reply Delay Request Message to Slave and Master sends Delay Response Message to Slave. Using timestamps these messages include Slave calculates Propagation Delay and Offset between Master and Slave as equation 3 and equation 4. Follow Up Message is used for passing on t_1 to Slave. Each message includes time-stamp and one way delay and offset are like following respectively. Hence, propagation delay and offset are calculated like following respectively.

$$D_{m2s} = t_2 - t_1 \quad (1)$$

$$D_{s2m} = t_4 - t_3 \quad (2)$$

$$\text{One way delay} = \frac{D_{m2s} + D_{s2m}}{2} = \frac{(t_2 - t_1) + (t_4 - t_3)}{2} \quad (3)$$

$$\text{Offset} = D_{m2s} - \text{One way delay} = \frac{(t_2 - t_1) - (t_4 - t_3)}{2} \quad (4)$$

where D_{m2s} is propagation delay from Master to Slave and D_{s2m} is that from Slave to Master. This calculate is followed as the servo diagram as Figure 2 [3] and it samples propagation delay between Master and Slave. This is based on equation 1 and equation 2.

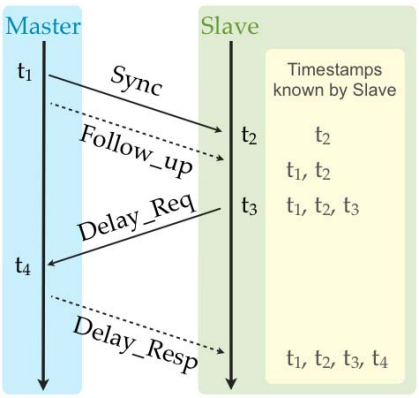

Figure 1. Message Exchange

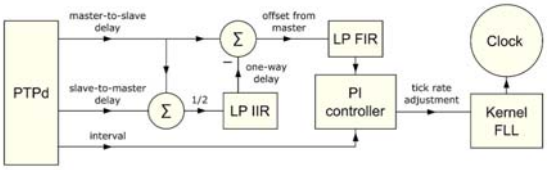

Figure 2. Clock Servo Diagram [3]

2.2 Effect of Asymmetric Network

It results of the calculation error of the offset between Master and Slave that D_{m2s} and D_{s2m} is different value. It is assumed that they are the same value in PTP and NTP like Equation 4. If D_{s2m} is equivalent with $D_{m2s} + \Delta\tau$, the offset is

calculated as following.

$$D' = D + \Delta\tau \quad (5)$$
$$t_2 - t_1 = D + O \quad (6)$$
$$t_4 - t_3 = D + \Delta\tau - O \quad (7)$$
$$O_m = \frac{(t_2 - t_1) - (t_4 - t_3)}{2} \quad (8)$$
$$= O - \frac{\Delta\tau}{2} \quad (9)$$

where D is D_{m2s}, D' is D_{s2m}, $\Delta\tau$ is the difference of D and D', O is the authentic offset, O_m is the measured offset, and t_1, t_2, t_3, t_4 are according to Figure 1. In the end $-\frac{\Delta\tau}{2}$ results in the calculation error of the offset.

2.3 Effect of Propagation Delay and Time Synchronization Interval

The offset is increasing during message exchanges. It is assumed that the propagation delay between Master and Slave is small enough for the offset calculation in NTP and PTP time synchronization, and it is responsible if it is done over the LAN. The larger propagation delay is, the larger the effect of time synchronization interval as followings.

$$O_i = O_{i-1} + A \cdot (t_4 - t_1) \quad (10)$$
$$O = O_m - A \cdot (t_4 - t_1) \quad (11)$$

where O_i is the calculated offset at the i-th time synchronization and A is the drift of Slave clock against Master. $A \cdot (t_4 - t_1)$ is the calculation error component of time synchronization.

3. Time Synchronization Experiment

3.1 Overview

We have made four experiments that are of PTP devices, M600/MRS and SyncBox made by Meinberg Radio Clocks Gmbh & Co. KG[2], and two computers using PTPd installed by "apt-get" command. M600/GPS and SyncBox are shown in Figure 3. M600/MRS has a role as Master and SyncBox has a role as Slave.

Note that the offset between the computers extends about 10^{-5} seconds per second. Hence the offset of such computers' is extending a few seconds per a day if each crock of a computer runs freely, and in this paper we call the time synchronization between M600/MRS and SyncBox as hardware time synchronization and that between computers as software clock synchronization for convenience.

Figure 3. The Experiment using M600/MRS and SyncBOX

3.2 over LAN

Figure 4 shows the network construction of these experiments over LAN. Two computers, M600/MRS, and SyncBox in which PTPd is running are connected over LAN of the laboratory of Yokohama National University and the synchronization interval of PTPd is 30 seconds.

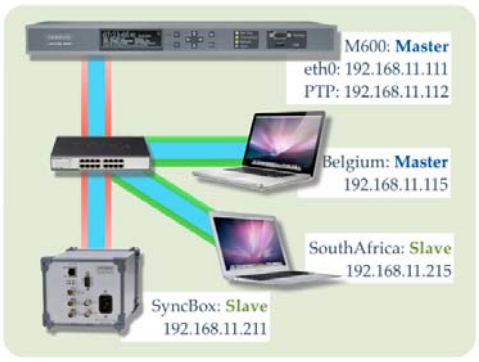

Figure 4. The Network Construction

Figure 5 shows the comparison of the time synchronization results using M600/MRS connected to SyncBox and computers over LAN.

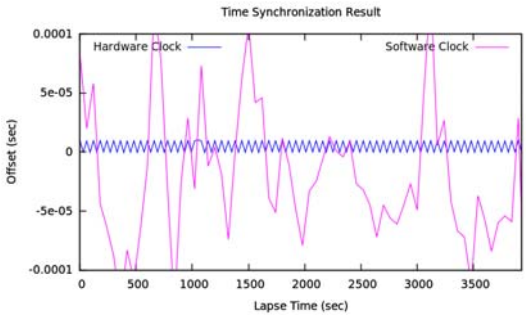

Figure 5. Offset Comparing over LAN

3.3 over VPN

Figure 6 shows that over VPN. M600/MRS and SyncBox are connected over VPN. In this situation Master is in the laboratory of Yokohama National University and Slave is in the room on the fifteenth floor of Yokohama Mitsui Building.

Figure 6. The Network Construction

Figure 7 shows the time synchronization result using M600/MRS connected to SyncBox over VPN.

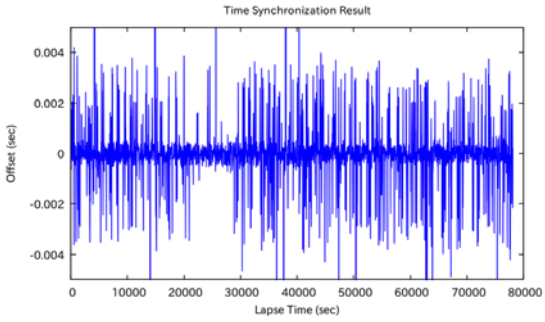

Figure 7. Offset over VPN

3.4 over WINDS

Figure 8 shows the network construction of the time synchronization experiment using WINDS that is the communication satellite launched by JAXA, Japan, 2008. It shows the top level bandwidth of Giga bit level and it has the function like a network switching hub for the effective data transfer of the long-distance e-Medicen and e-Education.

Figure 9[4] shows the time synchronization result using computers over WINDS network.

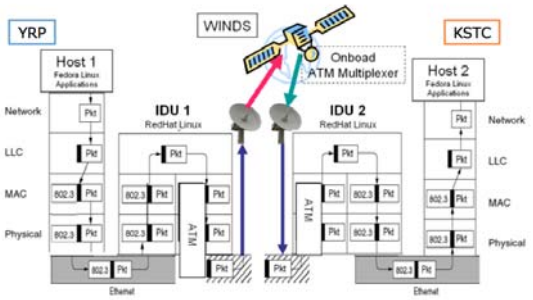

Figure 8. The Experiment through WINDS

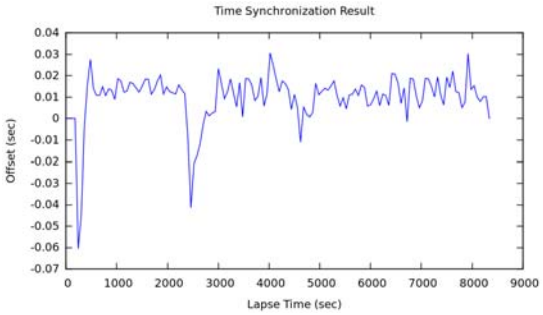

Figure 9. Offset over WINDS Network

3.5 Compiled Result

Table 1 and Table 2 are the compiled result of the above figures using LSM (Least Squares Method).

Table 1. Result Comparing

	Hardware Clock	
	over LAN	over VPN
Accuracy [sec/sec]	-2.78×10^{-12}	4.33×10^{-9}
Median [sec]	4.87×10^{-6}	2.70×10^{-4}
Variance [sec]	4.81×10^{-6}	8.22×10^{-2}

According to Table 1, the all parameters over VPN are worse than that over LAN. This means that the larger the propagation delay and the fluctuation component of that are, the larger these parameters are. Also according to Table 2, the all parameters over WINDS are worse than that over LAN. This results from the above, too.

4. Summary

We challenged and succeeded in the time synchronization over satellite network and VPN. In the result, the accuracy and the median of time

Table 2. Result Comparing

	Software Clock	
	over LAN	over WINDS
Accuracy [sec/sec]	-2.16×10^{-8}	-1.11×10^{-6}
Median [sec]	7.72×10^{-4}	5.07×10^{-3}
Variance [sec]	7.00×10^{-2}	1.15×10^{-2}

synchronization are influenced by the propagation delay, and the variance of that is influenced by the fluctuation component of the propagation delay. We will make the calibration system of the time synchronization calculation error resulted from that.

Acknowledgement

This experiment is supported by Takashi Takahashi, Toshio Asai, and Norihiko Katayama from NICT (National Institute of Information and Communications Technology). I would like to show my appreciation for them.

References

[1] "IEEE 1588-2008 Std.", IEEE 1588 Standard Board, 2008

[2] "Meinberg", http://www.meinbergglobal.com

[3] Kendall Correll, Nick Barendt, Michael Branicky: "Design Considerations for Software Only Implementations of the IEEE 1588 Precision Time Protocol", VTI Instruments, 2005,http://www.vtiinstruments.com

[4] Yusuke Kito Satoshi Kubota, Fujinobu Takahashi, Takashi Takahashi, Toshio Asai, Norihiko Katayama: "First Challenge of PTP Time Synchronization Experiment through the Experimental Satellite for Communication, "WINDS" ", ISAP 2012, 2012.11

Toward a Precise Frequency Comparison with VLBI Technique

Kazuhiro Takefuji (*takefuji@nict.go.jp*)[1], Mamoru Sekido, Hideki Ujihara, Thomas Hobiger, Masanori Tsutsumi, Shingo Hasegawa, Yuka Miyauchi, Ryuichi Ichikawa, Yasuhiro Koyama, and Tetsuro Kondo

[1] *Kashima Space Technology Center, National Institute of Information and Communications Technology, 893-1 Hirai, Kashima, Ibaraki 314-8501, Japan*

Abstract: We have been studying a frequency comparison technique using VLBI between distant stations. There are three important issues in our precise frequency comparison project with VLBI, one is the use of a efficient antenna and broad band receiver to obtain a good signal to noise ratio (SNR), second is a highly stable and reliable signal transfer, third is solving time delay caused by the ionosphere and the atmosphere. These three issues should be solved for precise frequency comparison by using a VLBI technique. This report describes some experiments to tackle to these issues.

1. Introduction

National Institute of Information and Communications Technology (NICT) has been not only developing VLBI observation system as the technology development center (TDC) of IVS, but also taking a role of authority maintaining the Japanese Standard Time (JST). Recently, the research on atomic clock improvement is rapidly in progresses in this field. NICT, National Institute of Advanced Industrial Science and Technology (AIST), and Tokyo University have been developing an optical-lattice clock for the next generation primary frequency standards and for the redefinition of "the Second". Thus, it is becoming important to compare the distant clocks with several techniques. If two stations are close in a few hundreds kilometer, frequency transfer with optical fiber link [2] will be the best way for that. However, for comparisons over inter-continental distances, techniques with space technologies such as GNSS, Two-Way Satellite Time and Frequency Transfer (TWSTFT) and VLBI are required.

Current target of the accuracy of comparison over long distance is in the order of 10^{-16} in a few days of interval. We will focus on more detail for the high precise comparison by the VLBI technique in this report.

2. Broadband System in the VGOS Era

For the next generation of the geodetic VLBI, VLBI2010 Global Observing System (VGOS) has specified a fast moving antenna and broad-band receivers. Some antennas, which meet with the VGOS requirements, have been constructed, for example GGAO 12m antenna, 18 meter Westford in the United States, TWIN Radio Telescope Wettezell (TTW) in Germany, the RAEGE telescope at Yebes in Spain, and Ishioka in Japan.

Now NICT/Kashima has also been developing a broad-band system for 3 GHz – 14 GHz frequency with the Kashima 34 meter diameter antenna and two small/transportable antennas. The broadband project is named "Gala-V"[1]. The system has some features different from other VGOS antenna. At first, a feed horn for the 34m antenna, which will be install until the end of this year, has a sharp beam of 12 degrees half-power beam width. Secondly a direct sampler, which has 16 GHz sampling speed, is going to be used instead of up-down converter. The direct sampler has four DBBC channels of 1 GHz bandwidth, which is tunable up to 16 GHz. Current Gala-V system is going to use fixed frequency array with 1 GHz bandwidth at 3.2 GHz, 4.8 GHz, 9.6 GHz, and 12.8 GHz. These frequency interval selection was decided with taking into account integer number of ratio 1:3:2 as the no-redundancy array, which enables fine delay resolution with minimum side-lobes.

3. For a Stable and Reliable Signal Transfer

VLBI observable is affected by variety of causes such as change of cable length of reference signal delivery from Hydrogen maser and change of characteristics of electronic components in the signal path from receiver to the sampler. Delay calibration signal (D-cal) and the phase calibration signal (P-cal) are used to calibrate the changes of the delays. The D-cal is used for monitoring the delay change of reference signal delivery to the P-cal, and P-cal is used for the delay calibration in the signal path to the sampler by injecting comb tone signal in front of a low noise amplifier.

The pseudo delay measurement result performed

at Koganei 11 meter antenna is shown in Figure 1. The pseudo delay was derived by Fourier transformation of the P-cal tones in 512 MHz band. That is equivalent with linear phase slope estimated by weighted least square. The magnitude of the variation was 80 pico second during about 4 hours. Figure 2 shows plot of temperature in the observation room at Koganei station, which shows fluctuations with about 20 minutes of period. The two figure indicating that the behavior of the pseudo delay coincides with that of room temperature. This periodic variation has not been awarded in the VLBI data analysis so far, although the cause of this should be investigated.

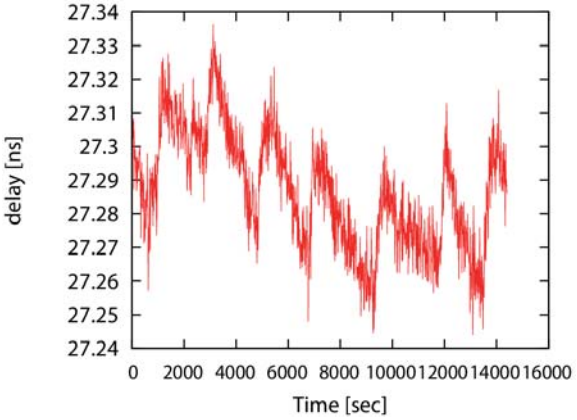

Figure 1. Variation of pseudo delay derived from P-cal tones over 512 MHz bandwidth in Koganei 11 meter antenna. Fluctuations with period of about 20 minutes are observed.

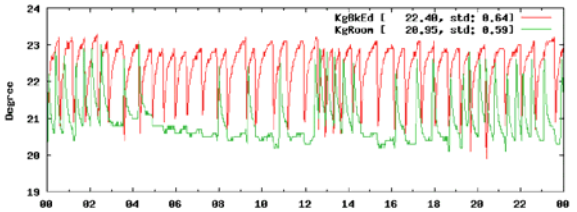

Figure 2. Temperature variation in the observation room of Koganei 11m station. Red and green line indicates thermal monitor sensor output located near the VLBI back-end and room air, respectively. Fast temperature variation (fast rising and slow decay) must be caused by air conditioner.

The Gala-V antennas are going to use P-cal device, originally designed by Haystack[3] and manufactured by A.E.S. Co. Ltd. Conventional P-cal uses 5/10 MHz reference signal, although we are going to use 50 MHz for reference input to the P-cal in our Gala-V system. A reason of using 50 MHz reference is to gain the power of P-cal signal at especially higher frequency. Generating uniform P-cal signal in the wide frequency range is essential for the system. We confirmed increasing the frequency interval from 10 MHz to 50 MHz enables generation of tone signal up to 15 GHz. Disadvantage of using 50 MHz reference signal is that P-cal signal does not always appear in 32 MHz bandwidth, which is supposed to be a basic observation mode in the VGOS. This is not the case for the Gala-V, where 1024 MHz bandwidth for a single channel. P-cal tone signal extraction is to be made via software correlator, and it will be used for delay calibration within the band.

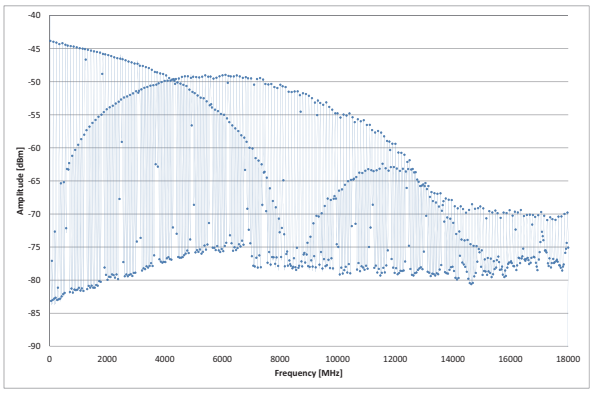

Figure 3. The comb tones of digital P-cal output in the case of 50 MHz reference input. Peak power of tone signals of 50 MHz interval and that of 100 MHz interval are exchanged along the frequency.

4. Fringe Phase for High Precision Delay Monitoring

As one of the approaches to get high precision delay observable, using fringe phase with tracking single radio source was examined. Table 1 shows parameters of fringe phase VLBI observation with tracking the 3C84. A purpose of the observation was to test extraction of ionospheric delay by using fringe phases, instead of combination of group

Table 1. Specifications of VLBI observation

Baseline	Kashima 11m and Koganei 11m
Source	3C84
Date	2013/100, 16 hours
Band	S/X (150 MHz / 512 MHz)
Record	1 Gsps, 1 bit, 2ch
Correlator	GICO3

delays at S-band and X-band which is used in the conventional geodetic VLBI.

There are four ways to obtain the ionospheric delay. One is to subtract the group delay among S/X band conventionally. The second is to take difference between the phase delays of S and X bands. However, it has only "relative" delay from initial one. The third uses an inverse feature between a phase delay and a group delay of X-band, and forth is the same with the third applied for S-band signal. The background theory of these features is described below. Phase velocity v_p is expressed by using a wave number k and an angular frequency ω as

$$v_p = \frac{\omega}{k}$$

It is also shown as

$$v_p = \frac{c}{n}$$

where c is the light speed in vacuum and n is a refractive index of medium. Thus,

$$\omega = kv_p = \frac{ck}{n}$$

Now we are thinking about the actual case in the ionosphere for the geodetic VLBI observations. In this case, ω is large enough compared with an angular cyclotron frequency in the ionosphere. Therefore n can be approximated by neglecting cyclotron frequency terms as

$$n = \sqrt{1 - \frac{\omega_p^2}{\omega^2}}$$

where ω_p is an angular plasma frequency and expressed as

$$\omega_p = \sqrt{\frac{\rho q^2}{\epsilon_0 m}}$$

where q, m, and ρ are the electron charge, mass, and density, and ϵ_0 is the dielectric constant in a vacuum. Hence

$$\omega = \frac{ck}{\sqrt{1 - \frac{\omega_p^2}{\omega^2}}}$$

Finally ω can be expressed as

$$\omega = \sqrt{c^2k^2 + \omega_p^2}$$

Then we get group velocity v_g as

$$\begin{aligned} v_g &= \frac{\partial \omega}{\partial k} \\ &= cn \end{aligned}$$

Ionospheric delay $\Delta\tau_{ion}$ can be derived from the difference of the phase delay and the group delay. Hence

$$\begin{aligned} \Delta\tau_{ion} &= \int_0^L \frac{dl}{v_g} - \int_0^L \frac{dl}{v_p} \\ &= \int_0^L \left(\frac{1}{v_g} - \frac{1}{v_p}\right) dl \\ &= \int_0^L \left(\frac{v_p - v_g}{v_p v_g}\right) dl \end{aligned}$$

Substituting $v_p v_g = c^2$,

$$\Delta\tau_{ion} = \frac{1}{c^2} \int_0^L (v_p - v_g)\, dl$$

On the other hand,

$$\begin{aligned} v_p - v_g &= c\left(\frac{1}{n} - n\right) \\ &= c\left(\frac{1}{\sqrt{1 - \frac{\omega_p^2}{\omega^2}}} - \sqrt{1 - \frac{\omega_p^2}{\omega^2}}\right) \end{aligned}$$

Assuming $\omega_p^2/\omega^2 \ll 1$, we get

$$\begin{aligned} v_p - v_g &= c\left(\left(1 + \frac{\omega_p^2}{2\omega^2}) - (1 - \frac{\omega_p^2}{2\omega^2}\right)\right) \\ &= c\frac{\omega_p^2}{\omega^2} \end{aligned}$$

Therefore

$$\begin{aligned} \Delta\tau_{ion} &= \frac{1}{c} \int_0^L \frac{\omega_p^2}{\omega^2} dl \\ &= \frac{q^2}{\epsilon_0 mc\omega^2} \int_0^L \rho dl \end{aligned}$$

Total electron content (TEC) is expressed by $\int_0^L \rho dl$, then we can get TEC as follows.

$$TEC = \frac{\epsilon_0 mc\omega^2}{q^2} \Delta\tau_{ion}$$

Figure 4 shows ionospheric delay contribution derived by four ways of the procedures described above. There are four combinations $S_g - X_g$, $S_p - X_p$, $S_p - S_g$, $X_p - X_g$, where S_g and X_g indicate the group delays of S and X-band, and S_p and X_p are the phase delays of those, respectively. Figure 5 shows the difference of total electron content (TEC) derived from the VLBI observation. Signal to noise ratio of TEC measurement was better in order of $(S_p - X_p)$, $(S_p - S_g)$,$(S_g - X_g)$, $(X_p - X_g)$. Thus, ionospheric delay variation can be monitored in best precision in the case using fringe phases. We will pursue precise measurement of the atmospheric delay by using the fringe phase also.

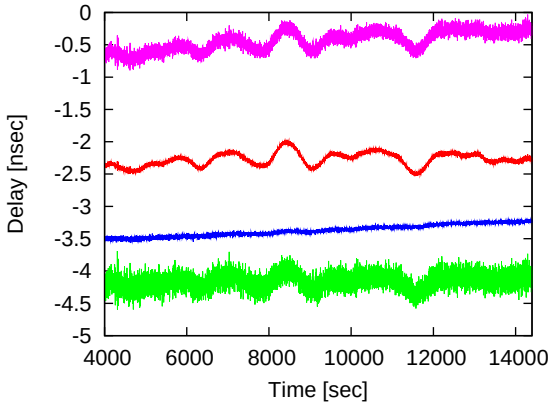

Figure 4. Ionospheric delay derived by four ways of procedures described in the main text. The lines of pink, red, blue, and green colors are plots of ionospheric delay derived by $(S_p - S_g)$, $(S_p - X_p)$, $(X_p - X_g)$, and $(S_g - X_g)$, respectively. The last one is the case of conventional VLBI. The lines have adequately offset to clearly seen.

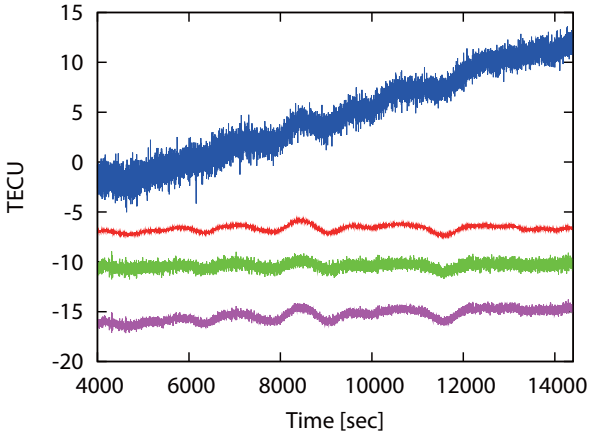

Figure 5. Total electron content (column density of electrons) derived by four ways of procedures. Vertical axis is indicated by TECU (10^{16} electrons/m^2). The lines of pink, red, blue, and green colors are plots of ionospheric delay derived by $(S_p - S_g)$, $(S_p - X_p)$, $(X_p - X_g)$, and $(S_g - X_g)$, respectively. The precision of the measurement is the best in the case using the phase delay difference between S and X band.

5. Summary

We have been investigating technique using VLBI for precise frequency comparison. Possible error source of delay fluctuations are examined with P-cal signal. For using P-cal in the broadband Gala-V system, we are preparing P-cal using 50 MHz reference signal. Also D-cal system via round-trip phase monitoring for 50 MHz reference signal is under investigation. As a trial to improve the measurement precision, we conducted the single radio source tracking experiment, and derived the ionospheric delay contribution in four ways of procedures. We confirmed that ionospheric delay variation could be monitored in better precision by using phase delay than the conventional group delay difference.

References

[1] M.Sekido, Development of Wide-band VLBI system (Gala-V), IVS NICT-TDC News No. 33, pp.11–14, 2013.

[2] M.Fujieda, M.Kumagai, S.Nagano, Coherent microwave transfer over a 204-km telecom fiber link by a cascaded system, IEEETUFFC, vol.57, no.1, pp.168-174, 2010.

[3] Rogers A.E.E.,Tests of new "digital" phase calibrator, MIT Haystack BBDev Memo#023, `http://www.haystack.mit.edu/geo/vlbi_td/BBDev/023.pdf`

Combination of space geodetic techniques on the observation level with c5++

Thomas Hobiger (*hobiger@nict.go.jp*) **and Toshimichi Otsubo**

National Institute of Information and Communications Technology
4-2-1 Nukui-Kitamachi, Koganei
184-8795 Tokyo
Japan

Geoscience Laboratory, Hitotsubashi University
2-1 Naka, Kunitachi
186-8601 Tokyo
Japan

Abstract: Multi-technique space geodetic analysis software has been developed which allows to combine data on the observation level. This novel concept is being tested with SLR, GPS and VLBI data. Results show that the combination of space geodetic data on the observation level leads to a consistent improvement of station position repeatability, Earth orientation parameters, etc. Furthermore, estimation of common parameters (troposphere or clocks) at co-located sites helps to improve the solution further and derive an utmost physically consistent model of the concerned parameters.

1. Introduction

Co-located space geodetic techniques can be found at so-called fundamental sites. At such stations two or more techniques are operated side by side and the reference points of the individual space geodetic instruments are connected by precise local tie measurements. Thus space geodetic data from different techniques can be combined for the purpose of reducing systematic (instrumental) effects. However, until now combination is mostly being done either on the level of normal equations or on the level of results. Even if space geodetic techniques are analyzed with the same geophysical and mathematical models, only a combination on the observation level can ensure a consistent usage of all observational data. Therefore, combination on the observation level is one of the goals for the realization of the Global Geodetic Observing System (GGOS) as described by Plag and Pearlman (2009).

2. Space geodetic data analysis with c5++

Driven by the need to update existing space geodetic analysis software and motivated by the demanding goals of GGOS, a new analysis package named "c5++" has been developed. After verification and comparison against other software packages, c5++ is currently being utilized for ultra-rapid determination of UT1 by means of Very Long Baseline Interferometry (VLBI) (Hobiger et al. (2010) and has been used to demonstrate the effect of combining Satellite Laser Ranging (SLR) and VLBI data on the observation level (Hobiger and Otsubo (2013a)). The modularity of this analysis software allows to process single technique solutions or combine the data on the observation level. As depicted in Figure 1, SLR, VLBI and Global Positioning System (GPS) modules share the same library which contains all geophysical models according to the latest IERS Conventions (Petit and Luzum (2010). In addition, local tie information can be included as virtual observations which relat e between the technique- specific reference points.

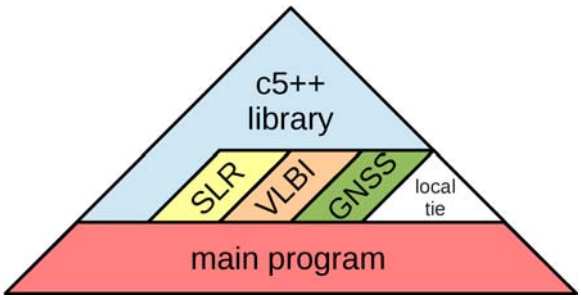

Figure 1. The basic concept of c5++ allows to process single- and multi-technique space geodetic observations by taking advantage from the usage of identical geophysical models.

2.1 Combination on the observation level

Other than combination of space geodetic results, where parameters are derived individually from each technique, combination of all available space geodetic observations on the observation level is expected to obtain more robust parameters. Outliers are less likely to bias the solution as data from other techniques helps to identify such data artifacts. Moreover, clock and troposphere parameters at co-located sites need to be estimated only once, which further stabilizes the geodetic solutions and avoids that data artifacts are absorbed in such nuisance parameters.

2.1.1 Prerequisites

Although combination on the observation level is straightforward with respect to the mathematical formulation, one needs to make sure that

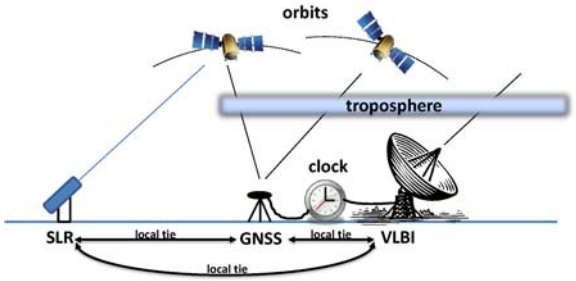

Figure 2. . Co-located space geodetic techniques and the possibilities for combining them directly(i.e. local-ties) or implicitly (i.e. by estimating common parameters).

the underlying (geo-)physical models are consistent among the different techniques. c5++ has been designed to ensure these requirements. However, estimation of a common troposphere model requires that a-priori hydrostatic delays are derived from consistent meteorologic data-sets. VLBI stations are usually equipped with ground meteo sensors, whereas such technology is not always deployed at GPS sites. Thus, VLBI meteo data has to be replaced with consistent meteorologic information which is also used for GPS processing and which allows to model the troposphere tie as a daily constant offset. This can be achieved by processing both, VLBI and GPS data, with the GPT2 model. Troposphere gradients can be assumed to be identical as long as the distance between the co-located techniques does not exceed a few kilometers, a criteria which is met at all fundamental sites. In addition to consistent a-priori models, one needs to make sure that inter-technique parameters are estimated with the proper temporal resolution. As discussed in the prior section, troposphere ties ΔD can be estimated as a constant offset over 24 hours. However, inter-technique clock differences $\Delta L(t)$ should be parameterized with a temporal resolution that allows to model at least a diurnal variation, which is the dominant signal caused by temperature dependent cable length variations.

2.1.2 Common parameters

Microwave based techniques like the Global Positioning System (GPS) or VLBI have in common that the neutral atmosphere (troposphere) causes signals to be delayed since the refractivity index of the gases in the media is not equal to one. Following Davis et al.(1993), one can model the troposphere excess delay for GPS in the form

$$\begin{aligned}\tau_{GPS} &= m_h(\varepsilon)D_{hz} + m_w(\varepsilon)D_{wz} \\ &\quad + m_g(\varepsilon)(G_N\cos\alpha + G_E\sin\alpha), \quad (1)\end{aligned}$$

where D_{hz} and D_{wz} are hydrostatic and wet zenith delays with the corresponding mapping functions $m_h(\varepsilon)$ and $m_w(\varepsilon)$ which depend on the elevation angle ε. Horizontal gradients in North- (G_N) and East-direction (G_E) allow to consider azimuthal (α) asymmetry and are mapped with a dedicated gradient mapping function $m_g(\varepsilon)$. Since hydrostatic delays can be computed a-priori with sufficient precision, one needs to estimate only wet zenith delays, respectively gradient parameters. If another microwave technique, e.g. VLBI, is co-located with the GPS antenna, one can assume that troposphere conditions are almost identical, i.e.

$$\tau_{VLBI}(\varepsilon) = \tau_{GPS}(\varepsilon) + m_h(\varepsilon)\Delta D \quad (2)$$

where the last term considers the height difference between the space geodetic instruments, which causes a small hydrostatic zenith delay ΔD. Estimating this so-called "troposphere-tie" as a daily constant value together with the other unknowns allows to obtain a single set of troposphere parameters for each space geodetic co-location site.
In addition, one can estimate a common clock model, if signals from a frequency standard are distributed to both systems, i.e. feeding the GPS receiver and steering the VLBI back-end. However, when expressing the relation between the VLBI and the GPS clock in the form

$$\text{clock}_{VLBI} = \text{clock}_{GPS} + \Delta L(t). \quad (3)$$

one needs to take into account that electrical cable lengths and VLBI equipment cause the offset term $\Delta L(t)$ to be time-dependent.
In contrary, combination of SLR and microwave based space geodetic techniques does not have any advantages for such nuissance parameters. However, if the same satellite is tracked by SLR and GPS, it is possible to estimate its orbit by combining the data from both techniques on the observation level. c5++ does not offer the possibility to estimate GPS orbits at the moment, but such a feature is expected to be implemented until the end of this fiscal year. Although combination of VLBI and SLR, as shown in section 3.2, does even have the possibility to estimate such common parameters, it is shown that the introduction of local-tie information alone is sufficent to improve the station coordinate estimates.

3. First results with c5++

In order to study the combination of space geodetic data on the observation level impacts the target parameters and helps to stabilize nuissance parameters, two different cases were studied. First, VLBI

and SLR data have been combined on the observation level at at single site, i.e. TIGO at Concepcion/Chile. In doing so, only local-tie information could be used to connect the two techniques. For the second test scenario, VLBI and GPS were combined, using the suggested common parameter set-up from section 2.1.2.

3.1 Combination of SLR and VLBI at TIGO

Fig. 3 shows the East component of the estimated SLR-only, VLBI-only and combined coordinate time series after the 2011 Earthquake, which shifts TIGO by almost 4 m westwards with respect to its original ITRF position. Both, formal errors and the scattering of the time series are significantly reduced when combining SLR and VLBI data. Thus, the underlying geophysical signal with its main component of a slowly decreasing Eastward plate velocity becomes very clear in the time series of the combined approach. SLR and VLBI results reveal a similar behavior, however the relatively large scattering between consecutive 10 day batches makes it difficult to see the exponential decrease of the post-seismic velocity. Although combination of space geodetic data improves the accuracy of the results, it happens that the estimate for the first 10 day batch in December 2010 can not be seen in the combined solution. A further discussion about this analysis and the impact of combination on the observation level on SLR and VLBI related parameters can be found in Hobiger and Otsubo (2013a).

3.2 Combination of GPS and VLBI during CONT11

In total 14 VLBI stations joined the CONT11, a campaign of continuous VLBI sessions observed between Sep. 15^{th} and Sep. 30^{th} 2011, network. However, since not all stations continuously contributed to CONT11 and only a fraction of the network station shared a common frequency standard with the co-located GPS receiver (Rieck et al. (2012)) only 7 stations remain which can be used for combination of GPS and VLBI. A VLBI-only (S0001) and a GPS-only PPP solution (S0010) were compute for reference. The first solution which combines GPS and VLBI on the observation level, i.e. S0011, only added local tie vectors as virtual observations that relate between the reference points of the co-located VLBI and GPS antennas. Taking this concept a step further leads to solution S0111, which includes the estimation of site-dependent troposphere parameters. The last solution (S1111) extends this approach further and deals with clock estimates as site-dependent parameters as well. In all solutions earth orientation parameters (EOPs), i.e. UT1 and pole coordinates (X_p/Y_p), were only estimated from VLBI data since GPS orbits were kept fixed. Station position repeatabilities, measured as root mean square (RMS) error, during the 15 day period are computed for each solution and then averaged over all network sites (Table 1). As expected, VLBI-only station position repeatability is worse than the GPS-only solution. In general, scattering of the VLBI-only solution is about twice as large as the GPS single-technique position results. However, once data are combined on the observation level and local tie vectors are added as virtual observations, co-located VLBI and GPS sites reveal the same stability. Estimating the troposphere conditions as site-dependent common parameters, as done in solution S0111, has another positive impact on the station position repeatability. T he estimation of both, common troposphere and clock parameters, as carried out in solution S1111, yields the best performance among all solution strategies. Table 2 summarizes the RMS of the EOP estimates w.r.t. the IERS-C04 time-series. It can be seen that solution S1111 performs much better than the VLBI-only analysis, showing an improvement in RMS of about 7 % RMS for UT1 as well as 37% and 23% for the pole coordinates respectively. An in-depth discussion of this results can be found in Hobiger and Otsubo (2013b).

Table 1. Mean station position repeatabilities (in mm) from the five different solutions (see text).

sol.	N/S	E/W	U/D	3D
S0001	2.74	4.65	8.11	9.97
S0010	1.46	2.35	4.12	5.12
S0011	1.40	2.24	4.00	4.95
S0111	1.33	2.13	3.93	4.82
S1111	1.28	2.07	3.97	4.81

Table 2. RMS of the differences between the estimated EOPs and those from the IERS-C04 time-series (see text).

sol.	UT1 [μsec]	X_p [μarcsec]	Y_p [μarcsec]
S0001	10.59	74.53	79.10
S0011	11.29	76.35	53.14
S0111	10.11	46.73	62.96
S1111	9.81	46.54	60.93

4. Discussion

It could be shown that combination of space geodetic data on the observation level improves both, geodetic target parameters and nuisance

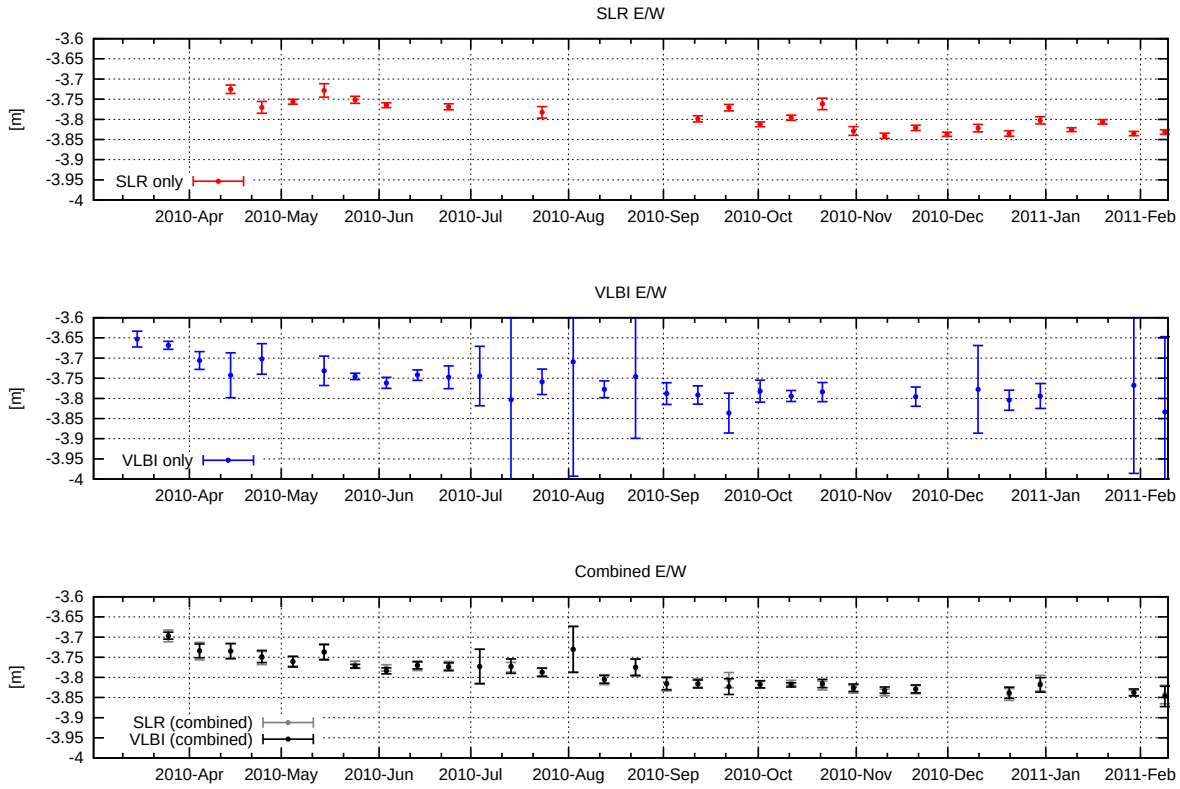

Figure 3. E/W components of post-seismic site displacements at TIGO from SLR-only, VLBI-only and combined solutions.

parameters like troposphere estimates. Parameters estimated from the combined approaches performed better than any of the single-technique solutions. In addition, outliers are less likely to mitigate into parameters when more than one space geodetic technique is used to estimate physically identical quantities like troposphere or clock offset. One can extend this concept and combine all three space geodetic techniques and estimate orbit parameters as well. In doing so, GPS satellites which are also tracked by SLR sites would increase the number of implicit links between the techniques and further improve the estimation of target parameters. Thus combination of space geodetic data on the observation level appears to be a promising strategy to support the GGOS goals and help to realize the next generation of reference frames which are requir ed for monitoring global change.

References

Davis J.L, G. Elgered, A.E. Niell, C.E. Kuehn (1993), Ground-based measurements of gradients in the "wet" radio refractivity of air, Radio Science, 28(6), 1003–1018

Hobiger T., T. Otsubo, M. Sekido, T. Gotoh, T. Kubooka, H. Takiguchi (2010), Fully automated VLBI analysis with c5++ for ultra-rapid determination of UT1, Earth Planets Space, 45(2), 75–79.

Hobiger T. and T. Otsubo (2013a), Observation Level Combination of SLR and VLBI with c5++: a case study for TIGO, submitted.

Hobiger T. and T. Otsubo (2013b), Combination of GPS and VLBI on the observation level — prerequisites, functional models and results, in preparation.

Petit G. and B. Luzum (2010), IERS Conventions (2010), IERS Technical Note 36, 179 pp.

Plag H.P. and M. Pearlman (2009), The Global Geodetic Observing System: Meeting the Requirements of a Global Society on a Changing Planet in 2020, Geoscience Books, Springer Berlin.

Rieck C., R. Haas, P. Jarlemark, K. Jaldehag (2012), VLBI frequency transfer using CONT11, European Frequency and Time Forum (EFTF), 163–165.

New Project for Constructing a VLBI2010 Antenna in Japan

Yoshihiro Fukuzaki (*fukuzaki@gsi.go.jp*), **Tadashi Tanabe, Jiro Kuroda, Shinobu Kurihara, Ryoji Kawabata, Takahiro Wakasugi**

Geospatial Information Authority of Japan
Kitasato-1, Tsukuba, Ibaraki, Japan

Abstract: The Geospatial Information Authority of Japan (GSI) has started a new project for constructing a VLBI2010 antenna (radio telescope) in Japan. The basic design of the specification of the antenna has been complete, and the antenna is now being constructed. The other equipments are almost complete and delivered to GSI. The observation system will be fully compliant with the VLBI2010 concept. The site candidate of the station for a new antenna is near Tsukuba. The antenna will be installed in the site by the end of this fiscal year.

The progress of the construction of the new antenna and the individual performance of the other equipments, which are already delivered to GSI, are briefly reported.

1. Introduction

The Geospatial Information Authority of Japan (GSI) has carried out VLBI observations since 1981. In the first period from 1981 to 1994, we developed transportable VLBI systems with a 5-m antenna and a 2.4-m antenna, and carried out domestic observations by using them. As a result, 8 sites in Japan were observed and precise positions determined. In addition, Japan-Korea VLBI observations were carried out by using a transportable 3.8-m antenna in 1995. In these observations, the Kashima 26-m antenna, which was removed in 2002, was used as a main station. Next, in the second period from 1994 to 1998, GSI established four permanent stations: Tsukuba 32-m, Sintotsukawa 3.8-m, Chichijima 10-m and Aira 10-m antennas. Up to the present, regular VLBI observations by using the four stations have been carried out. Especially, Tsukuba 32-m antenna is a main station for not only domestic but also international VLBI observations now.

In 2011, GSI started a project for constructing a new antenna following the VLBI2010 concept, which is recommended by the International VLBI Service for Geodesy and Astrometry (IVS) as the next-generation VLBI system.

This paper gives the outline of the project, the design specifications of the new antenna and the individual performance of the other equipments, especially analog devices, which are already complete.

2. Observing Facilities

In the new project, observing facilities will be constructed. The conceptual design consisting of the six components is depicted in Figure 1. The temporary operations room will be installed instead of the Operations Building.

3. Components

3.1 Antenna

The antenna (radio telescope) is the main part of the observing system. Since a single antenna will be employed, very high slew rates are specified in order to be compliant with the VLBI2010 concept. The design specifications of the antenna are listed in Table 1.

3.2 Front-end

According to the VLBI2010 concept, a wide-band feed is necessary to achieve high aperture efficiency over 2–14 GHz. At present the Eleven feed, which has been developed at Chalmers University of Technology in Sweden, is one of the practical for wide-band receiving. In addition, Quadruple-Ridged Fared Horn (QRFH), which has been developed by California Institute of Technology (Caltech), is also suitable for wide-band receiving. As a result, these two types of feeds are delivered to GSI. The employment of the feed will be determined after the evaluation of the antenna performance with these two feeds. For the design of the antenna optics, employing the Eleven feed is assumed.

The feed and Low Noise Amplifiers (LNAs) are integrated into the cryogenic system, whose physical temperature is less than 20K. The system noise temperature will be less than 40K (excluding atmospheric contributions).

Preliminary results of the measurements of the receiver noise temperature for QRFH system are shown in Figure 2. In the case of both polarizations, the noise temperature is almost less than 30K. (The spikes are caused by RFI.)

On the other hand, the Tri-band feed system will be installed by replacing the wide-band receiving system with it in order to perform legacy S/X band observations with Tsukuba 32-m antenna and the other legacy antennas.

The phase and cable calibration system will also be installed. A new type of P-cal unit is under development. In addition, instead of the present D-cal a new cable calibration system is also under

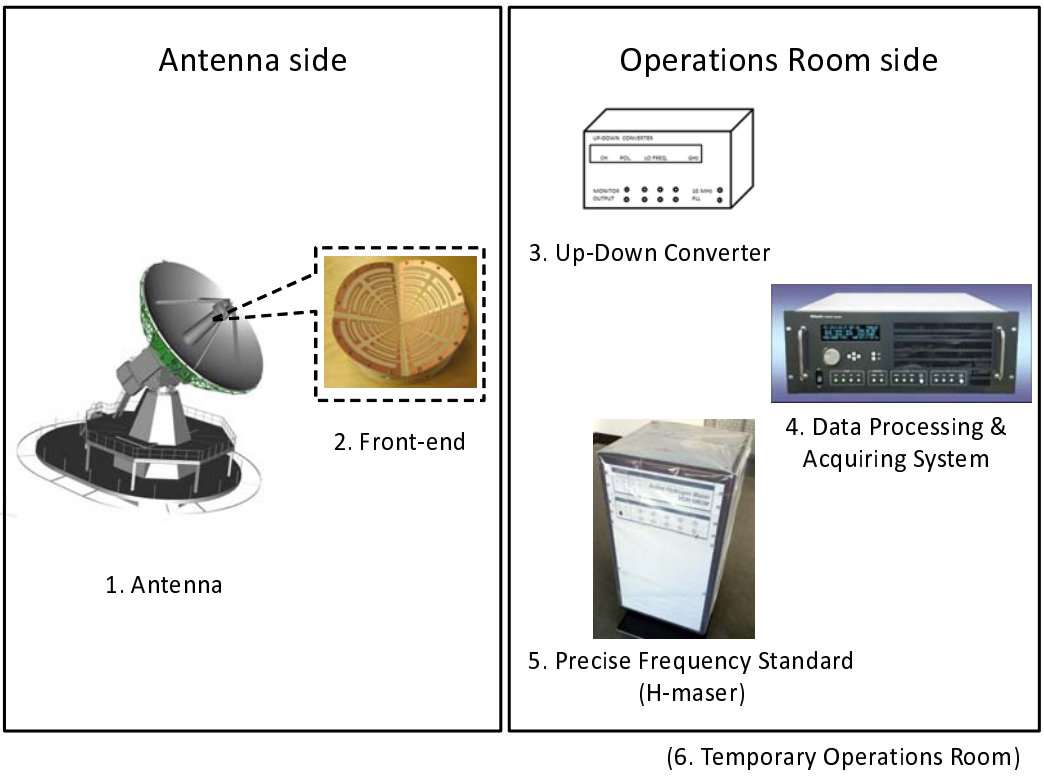

Figure 1. Conceptual design of the new observing facilities

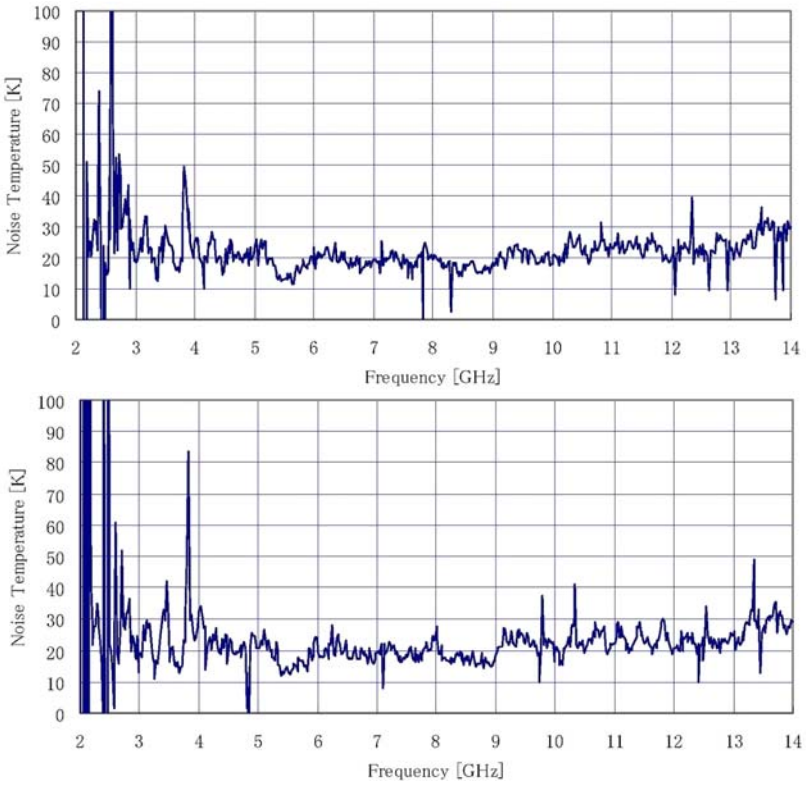

Figure 2. Receiver noise temperature for QRFH system (Upper: Horizontal polarization, Lower: Vertical polarization.)

Table 1. Design specifications of the new antenna.

Parameter	Value
Diameter	13.2 m
RF frequency range	2–14 GHz
Surface accuracy	$\leq$ 0.4 mm (rms)
Aperture efficiency	$\geq$ 50%
Antenna noise temperature	$\leq$ 10K (excluding atmospheric contributions)
System G/T	$\geq$ 45.882 dB (at 14 GHz) [T is the system noise temperature (Tsys), and Tsys excluding antenna noise temperature should be assumed as 30K.]
AZ maximum slew rate	$\geq$ 12°/sec
EL maximum slew rate	$\geq$ 6°/sec
AZ maximum acceleration rate	$\geq$ 3°/sec^2
EL maximum acceleration rate	$\geq$ 3°/sec^2
Cable for signal transfer	Optical fiber cable from antenna to building
Special feature	Reference point should be measured directly from the ground for co-location.

Table 2. Specifications of the front-end.

Parameter	Value
RF frequency range	2–14 GHz
Polarization	Dual linear polarization
Feed	Equivalent for Eleven feed or more
Dewar	Feed, LNAs, and other devices should be included and cooled by cryogenic system.
Physical temperature	$\leq$ 20K
System noise temperature	$\leq$ 30K (excluding antenna noise temperature)
Total gain	$\geq$ 45 dB
Output frequency range	2–14 GHz
Number of output	2 (for dual linear polarization)
Phase and delay calibration	New-type P-cal unit New cable calibration system developed by NICT
Injection of P-cal/noise-source	In the front of the feed

development. The specifications of the front-end are shown in Table 2.

3.3 Up-Down Converter

In order to convert the observed analog signal to digital data, the frequencies should be downconverted. For this purpose, a new Up-Down Converter is developed. The output signal frequencies are 1–2 GHz. The Lower Side Band (LSB) and Upper Side Band (USB) need to be selectable in the Up-Down Converter, because the second Nyquist zone will be used in the sampler (see *Kurihara* [2013]). The specifications of the Up-Down Converter are given in Table 3.

3.4 Additional Facilities

Optical fiber cables will be installed at the new site in order to establish a high-speed data link for data transmission. Initially, the transmission rate will be 10 Gbps; then it will be increased to 32 Gbps and more in the future.

A Global Navigation Satellite System (GNSS) continuous observation system will be installed at the new site to be registered as an IGS (International GNSS Service) station.

4. Candidate Site

The site candidate for a new station is near Tsukuba (about a 50-minutes drive by car). The

Table 3. Specifications of the Up-Down Converter.

Parameter	Value
Input frequency range	2–14 GHz
Output frequency range	1–2 GHz
Type of output signal	LSB or USB (selectable)
Number of units	4
Number of channel per one unit	2 (for dual linear polarization)
1st local oscillator	Programmable with 0.4-MHz step
2nd local oscillator	2 fixed LOs for LSB and USB
Total noise figure	$\leq$ 25 dB
Phase stability	$\leq 4^\circ$ with $\pm$ 2°C temperature change

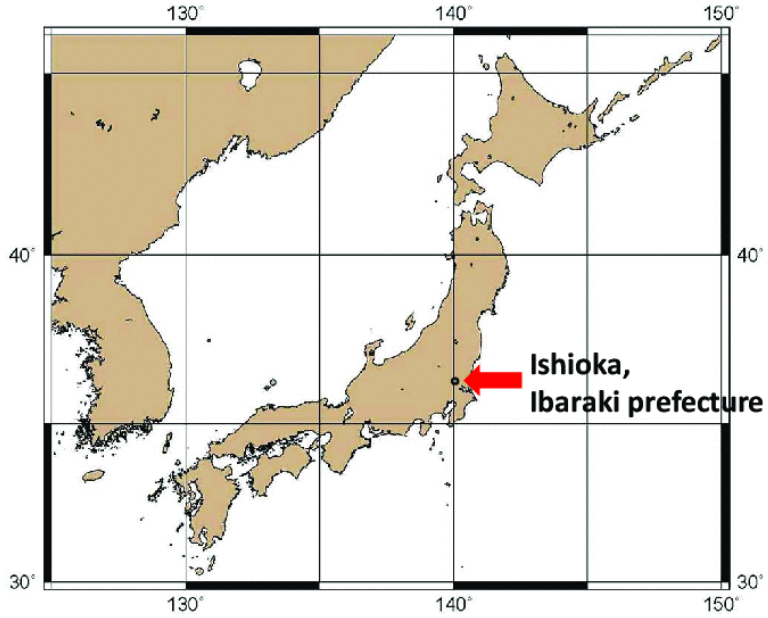

Figure 3. Location of the candidate site of the new observing facilities.

location is shown in Figure 3. According to the results of a soil investigation of the site, there is bedrock very close to the surface (at less than 3-m depth).

5. Summary

A new project for constructing a new antenna in Japan has started. The basic definition of the specifications has been accomplished. The new station will be fully compliant with the VLBI2010 concept. The construction of the station will be complete by the end of March 2013. After completion of the station, it will play an important role as a main station in the Asian region.

Reference

Kurihara S., VLBI2010 – Newly Established VLBI Station –, *IVS NICT Technology Development Center News*, No.33, pp.37–38, 2013.

VLBI2010 – Newly Established VLBI Station –

Shinobu Kurihara (*skuri@gsi.go.jp*)

Geospatial Information Authority of Japan
1 Kitasato, Tsukuba, Ibaraki 305-0811, Japan

Abstract: The Ishioka VGOS station is a newly established VLBI station of the Geospatial Information Authority of Japan. In this report, a set of the digital back-ends (DBE) together with a huge data storage system and a pair of hydrogen masers delivered by last March are briefly described. At the later half, the current situation of the construction and planning of VGOS staions in the world is reported.

1. Introduction

In 2011 fiscal year, the Geospatial Information Authority of Japan (GSI) decided to build a new VLBI2010 concept station. The International VLBI Service for Geodesy and Astrometry (IVS) named such a new station VGOS; VLBI2010 Global Observing System. The site of the Ishioka VGOS station is located 17 km northeast of the Tsukuba 32-m antenna, and the telescope will be built on a basement outcrop at the top of the small hill in the site of the Ibaraki Prefectural Livestock Research Center. The station will consist of a radio telescope, three alternative front-end systems, a flexible up-down converter (UDC), a set of the digital back-ends (DBE) together with a huge data storage system, and a pair of hydrogen masers. By the end of March 2013, all equipment except the antenna was already delivered to GSI. The DBE and hydrogen masers are reported in the next section. For the report of other equipment, see the article of Fukuzaki, et al. in this letter.

2. Delivered devices

2.1 Data Acquisition System

As a data acquisition system for VLBI2010 operation, a set of DBEs, Linux servers and a storage system was installed (Fig.1 and 2). The DBE is regarded as a successor of the Japanese VLBI systems like K4 and K5, and named as K6/iDAS (K6/Intelligent Data Acquisition and Streaming sampler). It is capable of 4-Gsps/2ch sampling with 8-bit quantization, DBBC function up to 32 channels with FPGA, and 4 Gbps/ch of maximum data rate by 10-GigE output. The 32-Gbps data rate that is a full VGOS recording (32 Gbps = 1-GHz bandwidth, 2 polarizations, 2 bit, and 4 channels) is available with four K6/iDAS units. The Linux servers and data storage system, which function as a recorder, are able to record 32-Gbps data stream from four DBEs without RAM buffer in

Figure 1. K6/iDAS sampler units in lack.

'burst mode' data acquisition. There is no removable disk; instead a 440-TByte total effective capacity RAID system is mounted for storage. Since Ishioka station will be linked to an external network with 10 GigE provided by SINET4, e-transfer is assumed for data transfer.

Figure 2. 18 Linux servers and a data storage system.

2.2 Hydrogen Maser

A pair of hydrogen masers VCH-1003M produced by the VREMYA-CH in Russia was delivered (Fig.3). They have 5, 10, 100, and 1400 MHz frequency standard output ports and two 1pps output ports. The frequency stability (allan deviation) is 2e-15 for 1000 sec. The frequency distributor, GPS receiver with Rb oscillator for time synchronization, remote monitoring and controlling system were developed and installed by a manufacturer in Japan. If one maser in operation has trouble, the other alternatively be switched from remote place by the remote controlling system. In preparation for power outage, the masers have the 12-hour UPS batteries.

Figure 3. Hydrogen masers and remote monitoring and controlling system.

3. VLBI2010 Situation in the World

Since the release of the progress report of VLBI2010 Committee of IVS [1], VGOS stations are being constructed and planned in many countries (Fig.4). In Germany, the Bundesamt für Kartographie und Geodäsie (BKG) completed the Twin Telescope Wettzell (TTW) with 13.2-m dishes. The inauguration ceremony was held on 26 April, 2013. The state secretary of Federal Ministry of the Interior, Cornelia Rogall-Grothe and the president of the BKG, Hansjörg Kutterer, and some guests were invited. Now a movie including fixed point photographing of its construction is available on the BKG website; `http://www.bkg.bund.de/nn_147094/DE/Aktu/01Meldungen/M2013/2013-04-30_Twin-Teleskope.html` (cited on June 11, 2013).

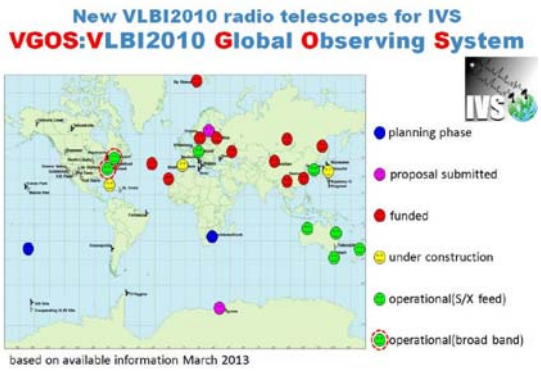

Figure 4. VGOS stations in the world as of March 2013.

The Instituto Geografico Nacional (IGN) in Spain is constructing a 13.2-m dish antenna at Yebes. It is a part of Spanish and Portuguese project RAEGE, and the Atlantic VLBI network will be completed with Santa Maria, Flores (Azores), and Tenerife (Canary Island).

In Russia as well, 4-station VGOS network is planned, and the construction will begin in 2015. The Shanghai Astronomical Observatory (SHAO) has obtained enough budget to construct three VGOS stations in China. The selected sites are Shanghai, Urumuqi, and Changchun. Other than that, Sweden and Norway are respectively planning the twin telescope construction. Many countries in the world are proceeding their VGOS project.

4. Summary

In the Ishioka VGOS station project, all equipment except the antenna was delivered by March 2013. We developed and installed the data acquisition system called K6/iDAS consistent with the full VGOS operation. Meanwhile, the construction of the telescope is ongoing. That will be completed by March 2014.

After the inauguration of the Twin Telescope Wettzell, many countries; Spain, Russia, China, Sweden, and Norway are proceeding the VGOS project in each country.

References

[1] Petrachenko, B., A. Niell, D. Behrend, B. Corey, J. Böhm, P. Charlot, A. Collioud, J. Gipson, R. Haas, T. Hobiger, Y. Koyama, D. MacMillan, Z. Malkin, T. Nilsson, A. Pany, G. Tuccari, A. Whitney, J. Wresnik, Design Aspects of the VLBI2010 System, Progress Report of the IVS VLBI2010 Committee, NASA Technical Memorandum NASA/TM-2009-214180, 2009.

Developments of K3, K4, and K5 VLBI Systems and Considerations for the new K6 VLBI System

Yasuhiro Koyama (*koyama@nict.go.jp*)

National Institute of Information and Communications Technology, 4-2-1 Nukui-Kitamachi, Koganei, Tokyo 184-8795, Japan

Abstract:

Historically, systems for VLBI observations and data analysis developed at Kashima Space Research Center have had codenames starting with the letter 'K'. Whereas K1 and K2 systems are experimental systems to demonstrate the capabilities of VLBI as an observation method, the successive series starting from K3 are practical systems routinely used for domestic and international VLBI sessions. In this report, the history of the developments of the K3, K4, and K5 VLBI systems are reviewed and considerations about the K6 VLBI system are presented.

1. Introduction

At Kashima Space Research Center of the National Institute of Information and Communications Technology (NICT), observation and data processing systems for VLBI have been designed and developed. In the 1980s, when the institute was called Radio Research Laboratories (RRL), the K3 VLBI system was developed as the first complete Japanese VLBI system to support both observations and data analyses. By using this system, global and domestic geodetic VLBI observations were performed under the Crustal Dynamics Project and other campaign projects conducted by international organizations or through institutional collaborations. The K3 VLBI system was adopted by Geospacial Information Authority of Japan (GSI), whose name was Geodetic Survey Institute at that time, and was used for more than 10 years for Geodetic and Astronomical VLBI observations at many VLBI observing stations in Japan. The developments of the K4 VLBI system were started in the late 1980's to expand the observation capabilities and to improve the operational functions. The K4 VLBI system was adopted by GSI, National Astronomical Observatory of Japan, National Institute of Polar Research, and Institute of Space and Astronautical Science (ISAS). NICT, at that time the name of the institute was Communications Research Laboratory (CRL), conducted Key Stone Project (KSP) from 1994 to 2001 and the developments of the K4 system were further performed. In the same period, ISAS conducted the VLBI Space Observatory Programme (VSOP) and used the K4 System for observations and data correlation processing. The developments of the K5 VLBI System were motivated by the idea to use conventional PC systems for data acquisition and correlation processing. The first K5 data sampler board and a group of software correlation programs were developed since 2001. The K5 VLBI Systems enabled VLBI observations and data analysis by smaller groups in universities and also stimulated the e-VLBI realtime/quasi-realtime observations over the public Internet. In this report, the characteristics and capabilities of the K3, K4, and K5 VLBI Systems will be reviewed, and in addition, the ideas and plans for new K6 VLBI System will be presented.

2. K3 VLBI System

The recording system of the K3 VLBI system was designed to maintain compatibility with the Mark-III VLBI system developed mainly by Haystack Observatory of the Massachusetts Institute of Technology in the United States. By using the K3 VLBI System, which is partially shown in the Figure 1, it became possible for the 26-m antenna VLBI station at Kashima to participate international geodetic VLBI sessions. Regular VLBI observations began from 1983 and it was soon confirmed that the distance between the Kashima 26-m VLBI station and the Kokee Park VLBI station in Kauai, Hawaii, USA, is decreasing due to the motion of the Pacific Plate with respect to the North American Plate. All of the systems necessary for VLBI observations were independently performed by the team in RRL with cooperation with Japanese vendor companies. Hydrogen maser system was developed to produce standard frequency signal to be used as a reference for frequency conversion of received signal, and for A/D sampling in the K3 Formatter. The longitudinal open-reel high speed recorder was designed to be compatible with the Mark-III recorder. This was, the data tapes recorded with the K3 Recorder could be read with the Mark-III Recorders at Collerator Centers in the United States of America and in Germany (Kunimori, et al., 1993).

3. K4 VLBI System

In the 1990s, a new VLBI observation and data processing system was developed as the K4 VLBI system. The developments were performed mainly under the Western Pacific VLBI Project which started in 1988 and the Key Stone Project which

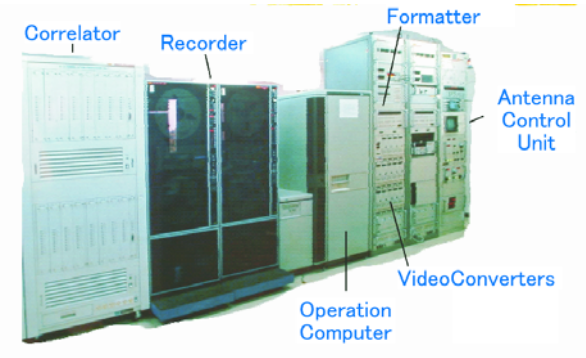

Figure 1. This picture shows observing part of the K3 VLBI System at observing station. The hydrogen-maser system for the frequency standard, correlator, data analysis and database systems are not shown in this picture.

started in 1994. The K4 VLBI system was designed to improve the sensitivity of the VLBI observations and the transportability of the system. For these purposes, a compact and high data rate recording system based on a helical scan recording head unit was adopted. The main concept of the developments of the K-4 VLBI observation and data analysis system was to minimize required human operations and to maximize operational reliability and durability. For the KSP VLBI Network system, a lot of technological challenges were made and realized. Figure 2 shows pictures of the K-4 observation system at observing stations and K-4 correlator system at Kashima Space Research Center.

The K-4 data recording system does not require frequent maintenance procedures and can record and reproduce observation data at the total data rates of 64 Mbps, 128 Mbps, and 256 Mbps with the bit error rate of less than 1×10^{-10} because of its robust error correction capability. The D-1 standard cassette tapes used to record the data are easy to handle and to transport. Using the tape changer unit with the K-4 data recorder unit, data recording can be continued up to 24 tapes which are equivalent to 20 continuous hours at the data rate of 256 Mbps. The correlation processing and the following data analysis procedures were also automated. Once the all observation tapes which were recorded during a VLBI session are set in the tape changer units of the correlator system, data correlation processing and data analysis are performed automatically without any human operations. With these systems, routine VLBI sessions were performed every day and the results of data analysis were placed on the WWW server within two days. Later in 1997, the data recording system was replaced with the high speed data transmission system using the high speed network and the real-time VLBI observations were realized (Kiuchi et al., 2000). With the real-time VLBI system, almost continuous observations at the data rate of 256 Mbps became possible and the analysis results were actually produced immediately after each observing session (Kondo et al., 1998). Since all procedures from the observation at the observing stations through the data analysis processing are completely automated (Koyama et al., 1998).

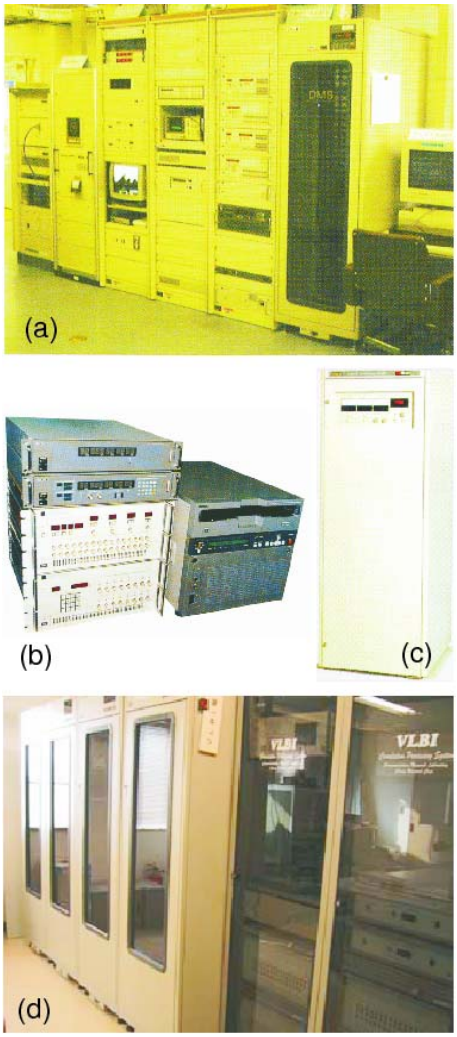

Figure 2. Pictures of the K4 VLBI Systems. (a) Observation parts of the K4 VLBI System at the observing station. (b) DIR1000 K4 recorder unit, DFC1100 Input Interface Unit, Video Converter Units and Local Oscillator Unit. (c) K4 hydrogen maser system. (d) K4 Correlator system for 4 stations 6 baselines.

After realizing high speed data sampling and data recording at 256 Mbps were achieved, further improvements were pursued by adopting giga-

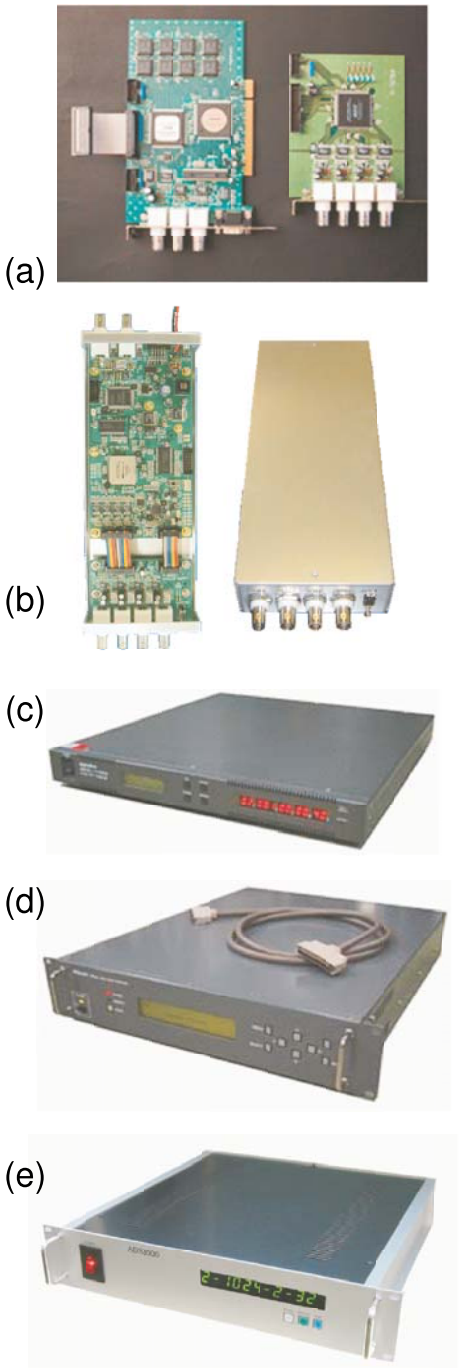

Figure 3. K5 VLBI Systems. (a) The initial version of the A/D sampling board K5/VSSP. (b) K5/VSSP32 system is interfaced with a PC running on Debian Linux operating system by a USB serial bus. (c) ADS1000 A/D sampler unit. (d) ADS2000 A/D sampler unit. (e) ADS3000 A/D sampler unit.

bit recorder unit GBR1000 based on the D6 cassette tape format. The GBR1000 recorder is interfaced to high speed sampler unit ADS1000 through the VLBI Standard Interface (VSI) specifications (Nakajima et al., 2001).

4. K5 VLBI System

In contrast to the K4 VLBI system, which was developed with the specially designed high-speed cassette tape recording system, the K5 VLBI system can be characterized as a system designed with the commodity products such as personal computers, hard disks, and network components. This strategy was quite successful since both high flexibility and high performance have been realized in the VLBI observation and data processing system. We have developed two independent series of systems as the data acquisition terminal of the K5 system as shown in the Figure 3. One is the K5/VSSP (versatile scientific sampling processor) system series (Kondo et al., 2003; Kondo et al., 2008) and the other is the K5/VSI system series (Koyama et al., 2003). The K5/VSSP system and its next generation K5/VSSP32 system comprised A/D sampling boards interfaced to the commodity PC systems by using the PCI (peripheral component interconnect) expansion bus (VSSP) and USB2.0 interface (VSSP32). Each A/D sampling board can support up to four analog inputs; therefore, four boards are used to record signals from 16 full channels of the baseband converter units for normal geodetic VLBI observations. On the other hand, the K5/VSI series is realized by high-speed A/D sampler units and all of the units interface with Linux PC systems with VSI-H specifications.

To input the data streams from the VSI-H compliant devices, such as the A/D sampler units, a special board called PC-VSI board was developed. The board is installed in the PCI-X expansion bus slot in a PC running Linux, and it can support high-speed data transfer and recording up to 2 Gbps with each board. By using two PC systems running Linux, each equipped with a PC-VSI board and a RAID controller board, a K5/VSI recording terminal can be configured. Since the K5/VSI recording terminal can record data streams input through a VSI data port, it is considered to be a DTS unit with only DIM capabilities. One K5/VSI recording terminal consists of two rack-mounted Linux operating PC units and necessary auxiliary components like an LCD (liquid crystal display) display, a keyboard, a mouse, and a switch for the components. Each PC unit is installed with a PC-VSI board and a RAID controller board on its PCI-X expansion bus slot. Sixteen 1 TB hard disks were connected to and controlled by each RAID controller board to configure the RAID-0 system. For one recording terminal, 32 TB of total data capacity was realized, and the data can be recorded

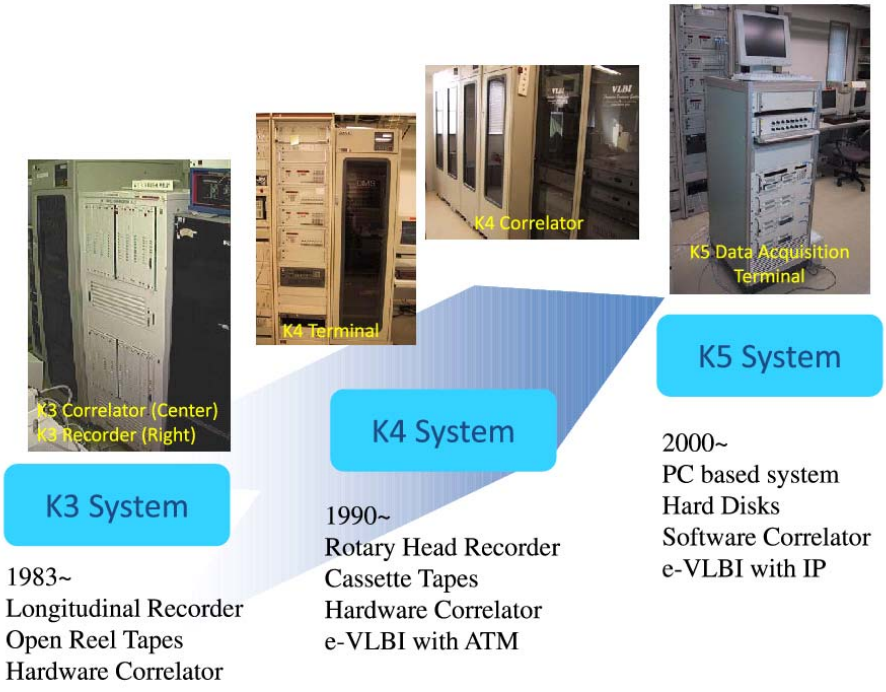

Figure 4. Evolutions of the VLBI Systems from K3 to K5.

at a maximum data rate of 4.096 Gbps by using two VSI-H data input ports. If the data are recorded continuously, the total capacity can support recordings for up to 17.36 hours. The capacity is considered sufficient for normal VLBI observations spanning 24 hours since the actual recording time is roughly 50% to 70% the total time for regular VLBI sessions. The capacity of the recording terminal can also be enlarged by replacing the hard disk units. Since the RAID controller board is used in a Linux PC environment, the data files can be easily accessed from application programs as simple data files on the Linux operating system.

5. Considerations for the new K6 VLBI System

As it is schematically shown in the Figure 4, K3, K4, and K5 VLBI systems were developed at Kashima Space Research Center roughly about every 10 years. These three systems have different concepts and characteristics as tabulated in the Table 1.

There were transition period between the systems and sometimes the various systems were used together. For example, the ADS1000 sampler unit has been used with the GBR1000 K4 recorder unit and K5/VSI PC recorder unit combined with the PC-VSI interface boards. Therefore, it may not be meaningful to categorize the individual systems into the K3, K4, and K5 categories. However, there are some key concepts which identify these systems. The concept of the K5 VLBI System is to utilize commodity systems and realize flexible data acquisition and data analysis. As the results, it became possible to adapt new developments into the existing systems and the it may not be necessary to considering the new concepts for next VLBI system with the codename of K6. However, it may also be adequate to launching a new project to develop new VLBI system since we need to design a new observing systems to realize VLBI2010. Obviously, we need to combine various efforts of multiple institutes since the requirements of the VLBI2010 system are all challenging. We need extremely high speed AD sampling, high volume data recording, high speed real-time filtering, high speed data transfer and correlation processing. Therefore, if we consider about the K6 VLBI System, its concept will be to realize VLBI2010 system. Members of GSI started to develop high speed data acquisition system under the codename of K6/iDAS. It will have an ample capability to realize VLBI2010 observations. In course of the various developments for VLBI2010, NICT, GSI, and other institutes will cooperate together to develop missing and unprecedented components under the codename of the K6 VLBI system.

References

Table 1. Comparisons of K3, K4, and K5 VLBI Systems.

	K3	K4	K5
Development Period	1979∼	1989∼	2000∼
Hydrogen Maser	◯	◯	—
Phase-cal & Delay-cal	◯	◯	—
A/D sampler & Recorder	∼56 Mbps	∼1024 Mbps	∼4096 Mbps
Correlator	Hardware	Hardware	Software
Data Analysis	◯	◯	◯
Key Concepts	International Compatibility	Automation Real-time	Commodity Versatility

Kiuchi, H., Imae, M., Kondo, T., Sekido, M., Hama, S. Hoshino, T., Uose, H., and Yamamoto, T., Real-time VLBI system using ATM network, IEEE Trans. Geosci. Remote Sensing, Vol.38, No.3, pp.1290-1297 (2000)

Kondo, T., Kurihara, N., Koyama, Y., Sekido, M., and Ichikawa, R., Evaluation of repeatability of baseline lengths in the VLBI network around the Tokyo metropolitan area, Geophys. Res. Let., Vol.25, No.7, pp.1047-1050 (1998)

Kondo, T., Y. Koyama, J. Nakajima, M. Sekido, and H. Osaki, Internet VLBI system based on the PC-VSSP (IP-VLBI) board, New Technologies in VLBI, ASP Conference Series, 306, 205-216 (2003)

Kondo, T., Y. Koyama, R. Ichikawa, M. Sekido, E. Kawai and M. Kimura, Development of the K5/VSSP System, J. Geod. Soc. Jpn., pp.233-248, Vol.54, No.4 (2008)

Koyama, Y., Kurihara, N., Kondo, T., Sekido, M., Takahashi, Y., Kiuchi, H., and Heki, K., Automated geodetic Very Long Baseline Interferometry observation and data analysis system, Earth, Planets, and Space, Vol.50, pp.709-722 (1998)

Koyama, Y., T. Kondo, M. Sekido, J. Nakajima, M. Kimura and H. Takeuchi, Adaption of the VLBI Standard Interface to the K5 VLBI System, J. Geod. Soc. Jpn., pp.249-258, Vol.54 No.4 (2008)

Kunimori, H., F. Takahashi, M. Imae, Y. Sugimoto, T. Yoshino, T. Kondo, K. Heki, S. Hama, Y. Takahashi, H. Takaba, H. Kiuchi, J. Amagai, N. Kurihara, H. Kuroiwa, A. Kaneko, Y. Koyama, and K. Yoshimura, Contributions and Activities of Communications Research Laboratory under the Cooperation with Crustal Dynamics Project, in Contributions of Space Geodesy to Geodynamics: Technology, eds. D. E. Smith and D. L. Turcotte, American Geophysical Union Geodynamics Series, Vol.25, pp.65-79 (1993)

Nakajima, J., Koyama, Y., Sekido, M., Kurihara, N., Kondo, T., Kimura, M., and Kawaguchi, N.: 1-Gbps VLBI, The first detection of fringes, Experimental Astronomy, Vol.11, pp.57-69 (2001)

Development of the Software Polarization Spectrometer "PolariS"

Izumi Mizuno[1,2] (*k7330312@kadai.jp*), **Seiji Kameno**[3], **Makoto Kuro**[1,4], **Amane Kano**[1], **Fumitaka Nakamura**[5], **Noriyuki Kawaguchi**[5], **Yoshiaki Hagiwara**[5], **Katsunori Shibata**[3], **Nario Kuno**[2], **Ryohei Kawabe**[3], **Shuro Takano**[2], **Daisuke Iono**[5], **Seisuke Kuji**[6]

[1] *Graduate School of Science and Engineering, Kagoshima University,1-21-35 Korimoto, Kagoshima, Kagoshima 890-0065*
[2] *Nobeyama Radio Observatory, Minamimaki, Minamisaku, Nagano, 384-1305, Japan*
[2] *Joint ALMA Observatory, Alonso de Cordova 3107 OFC 129, Vitacura, Chile*
[4] *Shoyo High School, Tatemachi, Hachioji, Tokyo 193-0944, Japan*
[5] *National Astronomical Observatory of Japan, Mitaka, Tokyo 181-8588, Japan*
[6] *Mizusawa VLBI Observatory, 2-12 Hoshigaoka-cho, Mizusawa, Oshu, Iwate 023-0861, Japan*

Abstract: We report the development of the software-based polarization spectrometer, PolariS, which aims the first detection of the Zeeman effect of the CCS emission line to measure the magnetic field in star-forming cores. This report addresses the specification, design, and performance of the PolariS in the commissioning phase.

1. Introduction

Polarization spectrometer is a device to measure spectra in full Stokes components of I, Q, U, and V. Stokes parameters in radio astronomy are essential to address magnetic fields in the emission region or along the propagation path. For example, the Zeeman effect is a key phenomenon to measure magnetic field strength directly. An emission line under a magnetic field shows frequency-shifted profiles due to energy level splitting. The Zeeman shift is proportional to the line-of-site magnetic field strength and opposite between two circular polarizations (LHCP and RHCP). Thus, Stokes V spectrum of the emission line is a concrete measure of the magnetic field strength.
The Zeeman effect of the CCS molecule is an important sensor for magnetic fields in star-forming cores. The emission line of $J_N = 4_3 - 3_2$ transition at 45.379 GHz is strong ($T_a \sim 2$ K), narrow (~ 0.5 km s^{-1}) and exhibit relatively large Zeeman splitting of 6.3×10^5 Hz G^{-1}[3]. In spite of some trials, however, no successful detection on CCS has been reported because of difficulties in measuring tiny Zeeman splitting in Stokes V.
We aim the first detection using the Nobeyama 45-m radio telescope which offeres the largest aperture at this frequency. We have developed a polarization spectrometer, "PolariS", together with a dual-polarization receiver for this purpose. In this paper we report the design of the PolariS and commissioning results.

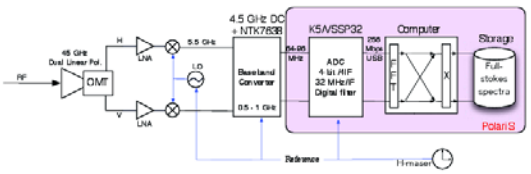

Figure 1. Schematic diagram of the PolariS and the receiving system of Z45 at the NRO 45-m telescope

2. Specifications and Design

For the purpose of CCS Zeeman observations, we set the technical requirements:

- Input : dual linearly polarized analog signal streams
- Output : Full Stokes (I, Q, U, V) spectra
- Bandwidth : 8 MHz to cover 50 km s^{-1}
- Resolution : 61 Hz for Zeeman shift of 100 μG
- Cost : $<$ JPY $2,000,000$

To meet the requirements, we designed a software-based spectrometer, PolariS. Figure 1 shows the schematic diagram of the PolariS. The input 4 IF signals are digitized with the K5/VSSP32 VLBI sampler[1] at 64 Msps 8-bit quantization. Digital filtering and level clipping is applied to output 4 data streams with each 16 Msps (8-MHz bandwidth) 4-bit quantization. The data streams are sent to the PolariS computer via USB 2.0 interface and processed for FFT (Fast Fourier Transform) and cross production in the GPU (Graphics Processing Unit) utilizing the CUDA (Compute Unified Device Architecture) library to output (cross) power spectra. The power spectra are accumulated for relevant period (typically 1 sec) and recorded in the storage. The operation software is open in the GitHub[1].

[1] https://github.com/kamenoseiji/PolariS

Figure 2. The front-inside view of the PolariS computer

We have four correlation pairs of $\langle XX^* \rangle$, $\langle XY^* \rangle$, $\langle YX^* \rangle$, and $\langle YY^* \rangle$ through the process, where X and Y stand for orthogonal linear polarizations, respectively. Each correlation pair contains 131072 spectral channels to offer the 61-Hz resolution. These pairs are related to the Stokes parameters:

$$\begin{pmatrix} I \\ Q \\ U \\ V \end{pmatrix} = \frac{1}{2} \begin{pmatrix} 1 & 0 & 0 & 1 \\ c & -s & -s & -c \\ s & c & c & -s \\ 0 & -i & i & 0 \end{pmatrix} \begin{pmatrix} \langle XX^* \rangle \\ \langle XY^* \rangle \\ \langle YX^* \rangle \\ \langle YY^* \rangle \end{pmatrix},$$

where $c = \cos 2\psi_{\rm m}$, $s = \sin 2\psi_{\rm m}$, and $\psi_{\rm m}$ is the parallactic angle. This conversion is employed in off-line reduction softwares.

Figure 2 shows the main body of the PolariS computer installed in the NRO. The computer costs JPY 70, 000 for the main body with the NVIDIA GT640 graphic card and operates on the Ubuntu 12.04 LTS. The total cost is JPY 600,000 including the ACD.

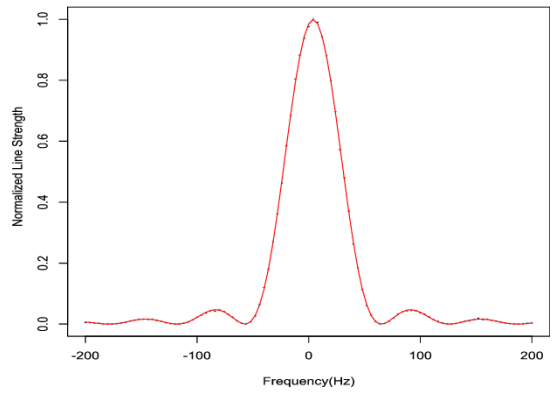

Figure 3. The spectral resolution of the PolariS. Measurements (dots) and best-fit Sinc^2 curve with the FWHM of 54.02 Hz (solid line) are displayed.

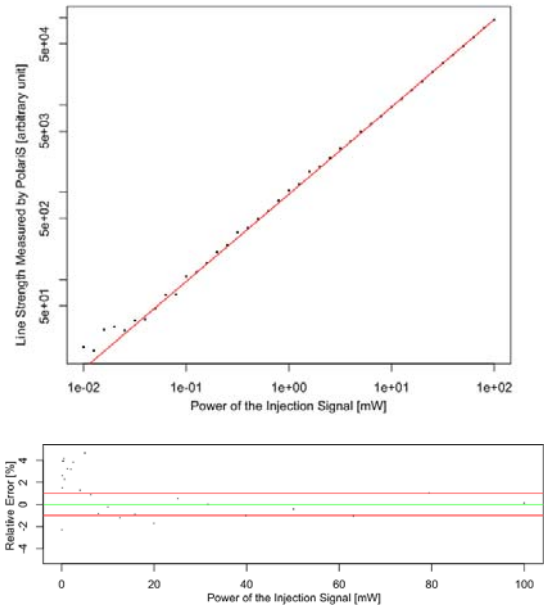

Figure 4. (Top) Line strength measured by the PolariS as a function of input power. (Bottom) Departure from the linear trend. Horizontal lines indicate the ±1% error range.

3. Commissioning Verification

We have tested the performance of the PolariS on the aspects: (1) spectral resolution, (2) linearity, (3) sensitivity, (4) stability, and (5) cross correlation capabilities. We used the Z45[2] and H22 receivers, working at 45 and 22 GHz, respectively, installed on the NRO 45-m telescope.

3.1 Spectral Resolution Function

Since the PolariS is a FX-type spectrometer with a triangular weighting function in an FFT segment of 262144 samples, we expect a Sinc-squared spectral resolution function with the FWHM of 54.07 Hz. To test the resolution, we prepared the baseband continuum signal from the Z45 receiver and injected a monochromatic signal at 68 MHz generated by the signal generator (Agilent E82579). The frequency was swept over the range of 400 Hz by a 4-Hz step. Figure 3 shows the measured resolution function, which follows Sinc^2 function with the FWHM of 54.02 Hz and consistent with the design.

3.2 Linearity

To verify the linearity in terms of spectral line intensity, we used the same configuration with subsection 3.1 and changed the power of the injection signal over the range of 41 dB by a 1-dB step.

Figure 4 shows that the departure from the linear trend is less than 1% in the range of 13 dB except a few outliers.

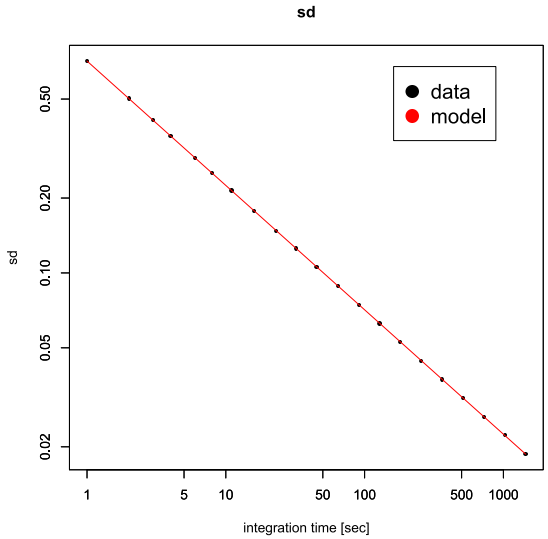

Figure 5. The standard deviation of the spectrum as a function of integration time.

3.3 Sensitivity

To evaluate the sensitivity, i.e. the standard deviation, σ, of the spectrum as a function of integration time, τ, we conducted spectroscopy of the Z45 signal under the shutter-closed circumstance. Figure 5 shows the results that well coincide to the ideal curve of $\sigma \propto \tau^{-1/2}$.

3.4 Stability

Using a long-term (2392 s) spectroscopy under the condition in subsection 3.3, we evaluated the flatness of the bandpass shape by taking the spectral Allan variance [4] and stability by the time-based Allan variance. As shown in Figure 6, the bandpass shape is flat for the channel separation of 7643 ch and stable over the time period of 1000 s.

3.5 Cross Correlation

To verify the cross correlation capability between orthogonal polarizations, we injected a linearly polarized wave from the calibration port of the H22 receiver which receives dual circular polarizations. The wave is generated by the signal generator (Agilent 83650L) and transmitted with a transducer with a rectangular waveguide. Thus, we expect 100% correlation with a constant relative phase for the ideal case. We show the results in Figure 7. The average of the cross correlation amplitude was

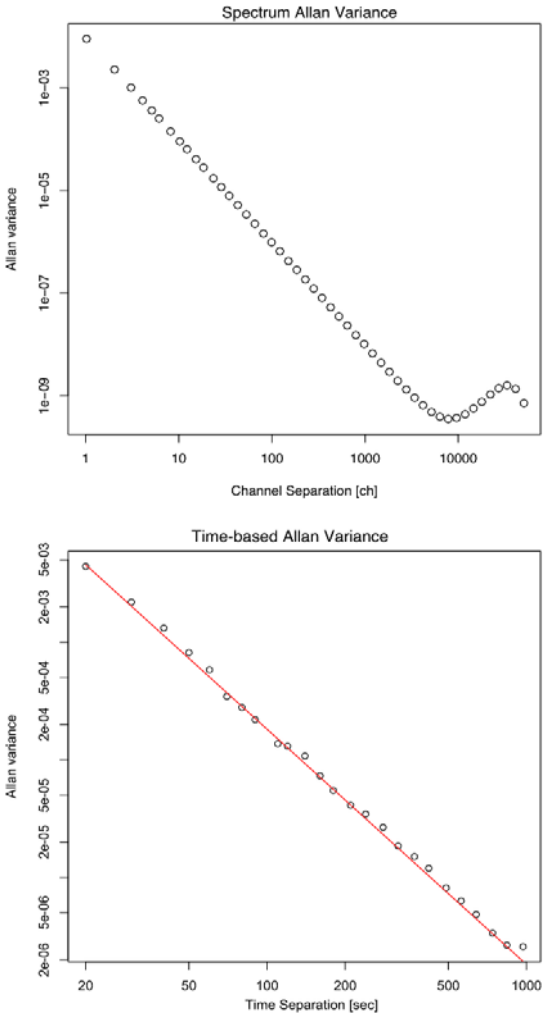

Figure 6. (Top) Spectral Allan variance of 2392-s integrated spectrum. The bandpass shape is flat until the first bottom of 7643 ch. (Bottom) Time-base Allan Variance together with the ideal curve in the solid line. The stability time exceeds 1000 s.

measured as $97.6 \pm 0.18\%$ and the phase was stable with the standard deviation of phase was $3^\circ.36$ during the 100-s observation.

4. Summary

Throughout the commissioning, we have verified the basic performance of the PolariS met the technical requirements for CCS Zeeman observations, in terms of spectral resolution, sensitivity, stability, and cross correlation capabilities. Since PolariS is a software-based equipment using commodity products, the radio astronomy community can easily install and utilize it or can contribute to improvements on specialized specifications.

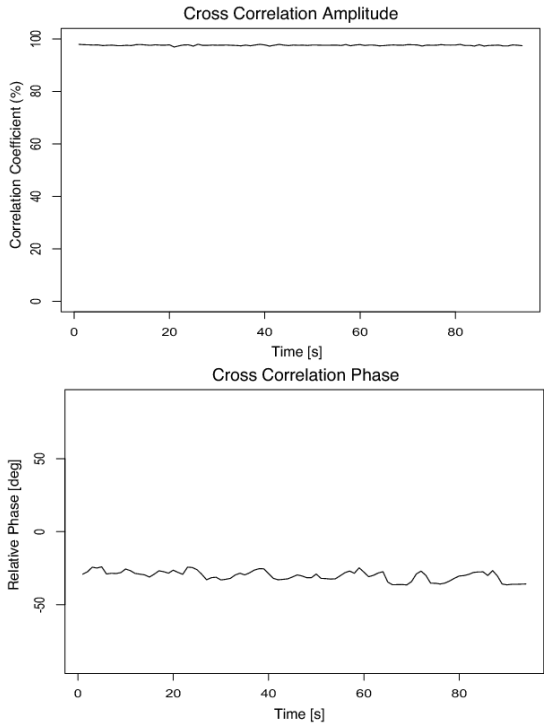

Figure 7. (Top) Correlation amplitude and (Bottom) phase across the elapsed time.

Acknowledgement

This project is financially supported by the joint development research program of the National Astronomical Observatory of Japan. The Z45 receiver is developed through the Grants-in-Aid for Scientific Research Program 24244017.

References

[1] Kondo, T., Koyama, Y., Takeuchi, H., & Kimura M. 2006, Proceedings of the IVS 2006 General Meeting, 195

[2] Kozu, M. et al. 2012, Annual Meeting of the Astronomical Aociety of Japan, V106b.

[3] Shinnaga, H., & Yamamoto, S. 2000, ApJ, 544, 330

[4] Yamaki, H., Kameno, S., Beppu, H., Mizuno, I., & Imai, H. 2012, PASJ, 64, 118

~ News ~ News ~ News ~ News ~ News ~ News ~ News ~ News ~ News ~

Restoration of 34m Antenna Azimuthal Wheel/Rail from the Damage of the Earthquake 2011

Kashima area was suffered from the "2011 Tohoku Megaquake"[1]. The damage to the 34m antenna was initially thought to be not so hard, although a large crack on the running surface of the azimuthal wheel has been found in the later inspection. Then detailed inspection was made by the original manufacturer General Dynamics SATCOM Technologies (originally 'TIW') in May 2012. Four azimuthal wheels and 16 wear-strip plates (Azimuthal rail) were replaced with new ones by the end of March 2013. Precision of the installation of azimuthal wear-strip plates was 0.1 mm height over the whole 20 m diameter azimuth rail circle. The installation of azimuthal wheel was performed with axis alignment at 10^{-6} radians of precision to the center of the azimuthal circle. Fig. 1 shows pictures of the damage on the azimuthal wheel surface and installation of a new wheel. Now, Kashima-34m VLBI station has been fully restored from the damage of the earthquake. It has started participation to the international IVS sessions and domestic VLBI sessions. Moreover, this antenna will become one of the keys in the Gala-V project[2], which is the mission of VLBI group at NICT/Kashima.

Figure 1. Left panel shows the crack on the wheel with 20cm/7.5cm size. Right panel indicates the installation of new wheel, whose axis is accurately aligned to the center of the azimuthal axis by using a telescope.

References

[1] Ichikawa Ryuichi, Preface, IVS NICT-TDC News, No. 32, pp.1–4, 2013.

[2] Mamoru Sekido, et al., Development of Wide-band VLBI system (Gala-V), IVS NICT-TDC News, No. 33, pp.11–14, 2013.

(Mamoru Sekido, Eiji Kawai/NICT Kashima)

"IVS NICT Technology Development Center News" (IVS NICT-TDC News) published by the National Institute of Information and Communications Technology (NICT) (former the Communications Research Laboratory (CRL)) is the continuation of "IVS CRL Technology Development Center News" (IVS CRL-TDC News). (On April 1, 2004, Communications Research Laboratory (CRL) and Telecommunications Advancement Organization of JAPAN (TAO) were reorganized as "National Institute of Information and Communications Technology (NICT)".)

VLBI Technology Development Center (TDC) at NICT is supposed

1) to develop new observation techniques and new systems for advanced Earth's rotation observations by VLBI and other space techniques,
2) to promote research in Earth rotation using VLBI,
3) to distribute new VLBI technology,
4) to contribute the standardization of VLBI interface, and
5) to deploy the real-time VLBI technique.

The NICT TDC newsletter (IVS NICT-TDC News) is published annually by NICT.

This news was edited by Mamoru SEKIDO, Kashima Space Technology Center. Inquires on this issue should be addressed to Mamoru SEKIDO, Kashima Space Technology Center, National Institute of Information and Communications Technology, 893-1 Hirai, Kashima, Ibaraki 314-8501, Japan, e-mail : sekido@nict.go.jp.

Summaries of VLBI and related activities at the National Institute of Information and Communications Technology are on the Web. The URL to view the home page of the Radio Astronomy Applications Section of the Space-Time Measurement Group of Space-Time Standards Laboratory is : **"http://www2.nict.go.jp/aeri/sts/stmg/index_e.html"**.

IVS NICT TECHNOLOGY DEVELOPMENT CENTER NEWS No.33, September 2013

International VLBI Service for Geodesy and Astrometry
NICT Technology Development Center News
published by
National Institute of Information and Communications Technology, 4-2-1 Nukui-kita, Koganei, Tokyo 184-8795, Japan